Journal of Medicinal Chemistry

Article

pubs.acs.org/jmc

Diazine Indole Acetic Acids as Potent, Selective, and Orally Bioavailable Antagonists of Chemoattractant Receptor Homologous Molecule Expressed on Th2 Cells (CRTH2) for the Treatment of Allergic Inflammatory Diseases

Neelu Kaila,* Adrian Huang, Alessandro Moretto, Bruce Follows, Kristin Janz, Michael Lowe, Jennifer Thomason, Tarek S. Mansour, Cedric Hubeau, Karen Page, Paul Morgan, Susan Fish, Xin Xu, Cara Williams, and Eddine Saiah

BioTherapeutics Chemistry, Pfizer Worldwide Medicinal Chemistry, 200 Cambridgepark Drive, Cambridge, Massachusetts 02140, United States

ABSTRACT: New classes of CRTH2 antagonists, the pyridazine linker containing indole acetic acids, are described. The initial hit **1** had good potency but poor permeability, metabolic stability, and PK. Initial optimization led to compounds of type **2** with low oxidative metabolism but poor oral bioavailability. Poor permeability was identified as a liability for these compounds. Addition of a linker between the indole and diazine moieties afforded a series with good potency, low rates of metabolism, moderate permeability, and good oral bioavailability in rodents. **32** was identified as the development track candidate. It was potent in cell based, binding, and whole blood assays and exhibited good PK profile. It was efficacious in mouse models of contact hypersensitivity (1 mg/kg b.i.d.) and house dust (20 mg/kg q.d.) when dosed orally. In sheep asthma, administration at 1 mg/kg iv completely blocked the LAR and AHR and attenuated the EAR phase.

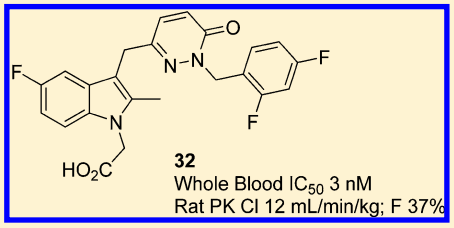

INTRODUCTION

Chemoattractant receptor homologous molecule expressed on Th2 cells (CRTH2) is a seven transmembrane, Gi coupled receptor expressed on Th2 cells, eosinophils, basophils, and monocytes.[1] CRTH2 is a rather promiscuous receptor binding to prostaglandin D2 (PGD2) and several of its metabolites as well as a number of prostaglandin D (PGD) synthase independent prostaglandins including 11-dehydrothromboxane B2 (TXB2), a metabolite of thromboxane A2 (TXA2), and of prostaglandin F2α (PGF2α). Signaling through CRTH2 attenuates adenyl cyclase (AC) activity through Giα coupled proteins, resulting in a decline in intracellular cAMP levels and a rise in intracellular calcium levels that leads to T cell, eosinophil, basophil, and monocyte chemotaxis as well as stimulation of TH2 T cell cytokine production. PGD2 is the major prostanoid produced by mast cells, a key cell type involved in the pathogenesis of allergic inflammatory diseases. Following activation of mast cells via IgE/allergen cross-linkage, cytosolic phospholipase A2 (cPLA2) translocates to the membrane, leading to the release of arachidonic acid (AA).[2,3] AA is further metabolized via cycloxygenase and PGD synthase to produce PGD2. PGD2 can then bind to either the prostaglandin D2 receptor DP1 or CRTH2 (prostaglandin D2 receptor, DP2) to induce multiple proinflammatory sequelae, resulting in chronic tissue inflammation. Importantly, blood eosinophilic CRTH2 expression is significantly increased in atopic dermatitis patients and is directly correlated with increased clinical severity score.[1c,4] Furthermore, single nucleotide polymorphisms in the CRTH2 gene have been linked to increased risk of allergy/asthma. These data strongly implicate the PGD2/CRTH2 signaling pathway in allergic disease.[5] Several companies have taken CRTH2 antagonists into clinical trials for treatment of allergic rhinitis, asthma, and COPD.[6] Most advanced are Oxagen and Actelion who have reported positive results in preliminary phase II studies. The Oxagen compound shows a significant increase in forced expiratory volume in 1 s (FEV1) and reduction in IgE and in sputum eosinophilia at a 100 mg twice daily dose.[7] Actelion has reported a positive proof-of-mechanism study with its orally active CRTH2 antagonist demonstrating efficacy on the primary end-point (FEV1) during the late allergic reaction (3−10 h) after a bronchial allergen challenge.[8] Recently Actelion also reported that its compound met its primary end-point in seasonal allergic rhinitis. In addition AstraZeneca has reported successful completion of phase II studies with 4-(acetylamino)-3-[(4-chlorophenyl)thio]-2-methyl-1*H*-indole-1-acetic acid (AZD1981) for treatment of COPD.[9] Novartis clinical candidate is being evaluated in two clinical trials for safety and efficacy in asthma patients.[10] Amgen is evaluating a CRTH2/DP dual inhibitor in a 12-week clinical trial at a once a day dose of 200 mg and twice daily doses of 100, 25, and 5 mg.[11] Actimis is testing its compound in phase I clinical trials.[12]

Recently, Amira has announced successful completion of phase 1 trials with a dose proportional pharmacodynamic effect with two candidates. The first is 2-(2′-((3-benzyl-1-

Received: January 3, 2012

 © XXXX American Chemical Society

Scheme 1. Synthesis of Diazine Indole Acetic Acids

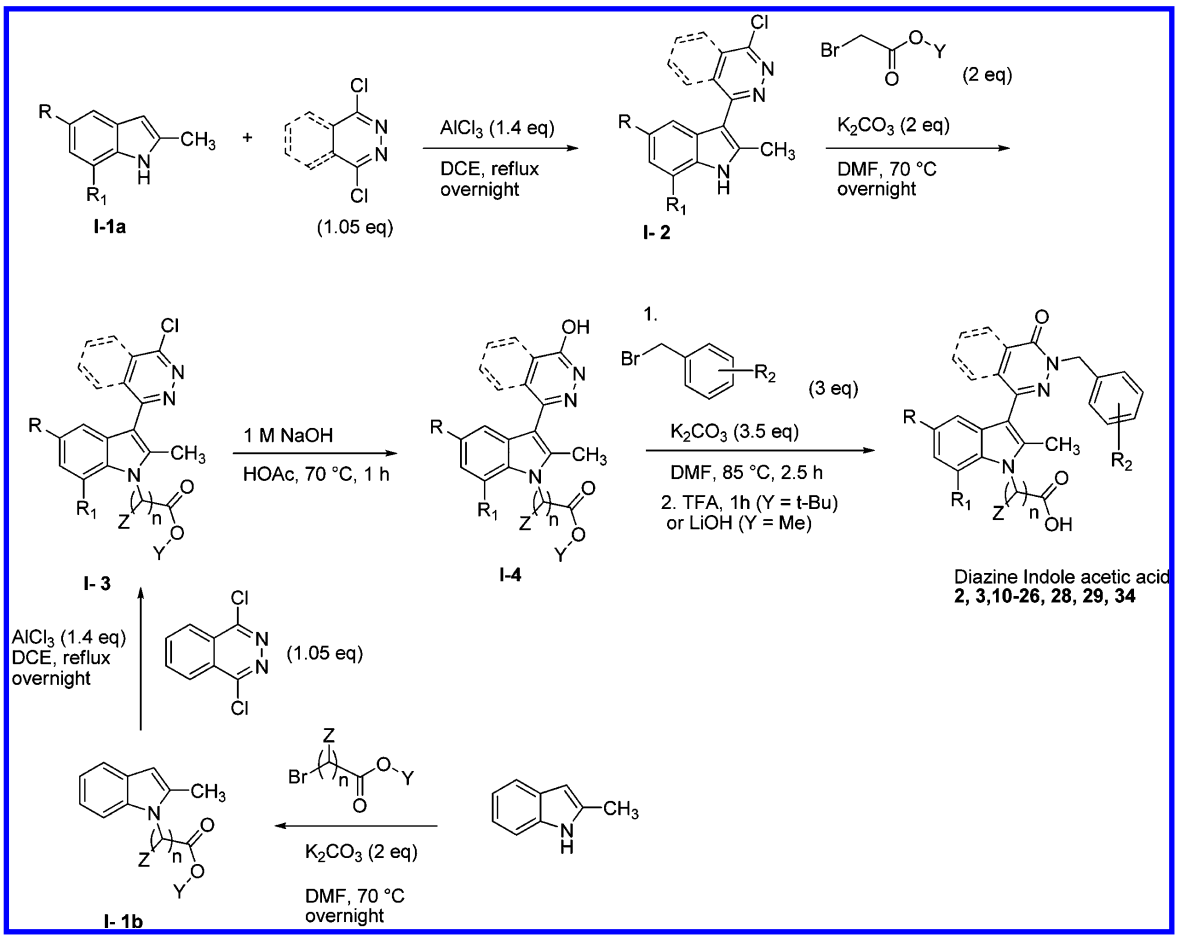

Scheme 2. Synthesis of 5,6-Disubstituted Indoles

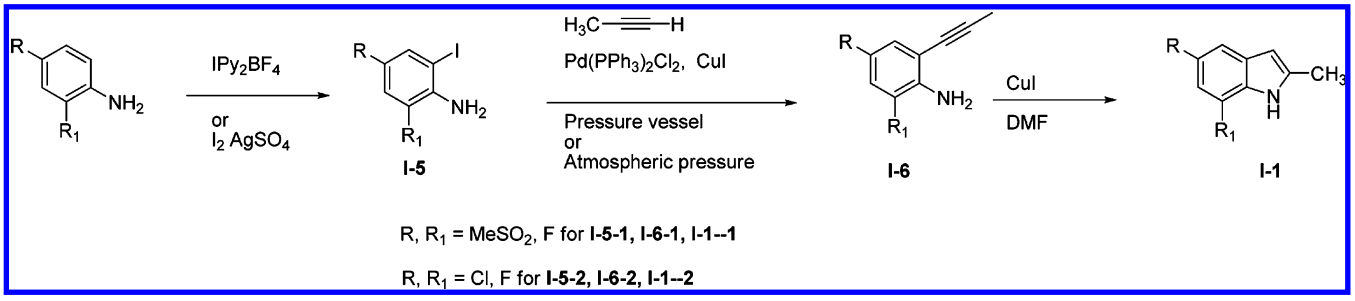

ethylureido)methyl)-6-methoxy-4′-(trifluoromethyl)biphenyl-3-yl)acetic acid (AM211), and the details for the second compound have not been disclosed.[13]

Successful clinical results in the past few years have stimulated interest in discovering potent, selective, and orally active CRTH2 antagonists for the treatment of asthma. Arylacetic acid is a common motif for a large number of CRTH2 antagonists reported in the literature.[6,14] Our starting point was diazine indole acetic acids.[15] A cAMP cell based competitive immunoassay (hCRTH2 FRET) using Eu^{3+} cryptate labeled anti-cAMP and d2-labeled cAMP was used as a primary in vitro screen. The lead compounds from a limited set of analogues made in this series showed good potency in the FRET assay but had high molecular weight and clogP and poor microsomal stability. The most potent compound in the series was **1** with IC_{50} = 2 nM in the FRET assay. A pharmacokinetic (PK) study of **1** showed poor bioavailability and high total clearance in mice. Its in vitro metabolic stability in mouse liver microsomes was low. In this article we describe the design and synthesis of novel compounds based on modifications to **1**.

■ CHEMISTRY

The 3-diazine-substituted indole acetic acids (**2**−**26**, **28**, **29**, **34**) were synthesized by the method reported by Pal et al.[16] through aluminum chloride induced C−C bond formation (Scheme 1). Reaction of **2**-methylindole (**I-1**) with dichlorodiazine under Friedel−Crafts reaction conditions gave chlorodiazineindole (**I-2**), which was converted to indole-*N*-acetic acid ester (**I-3**) upon reaction with bromoacetate. The latter was converted to the corresponding diazinones (**I-4**) using sodium acetate in acetic acid under reflux conditions. Diversification was then possible by introduction of substituted benzyl groups in the presence of potassium carbonate in DMF

Scheme 3

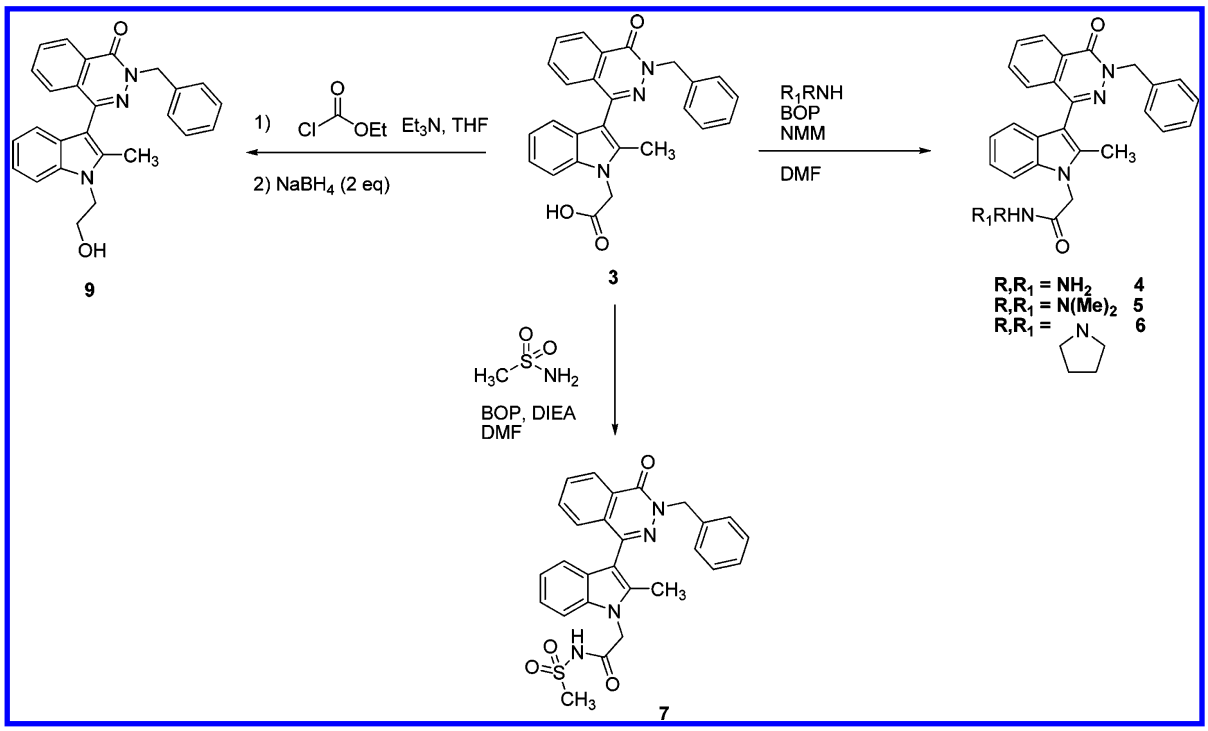

Scheme 4

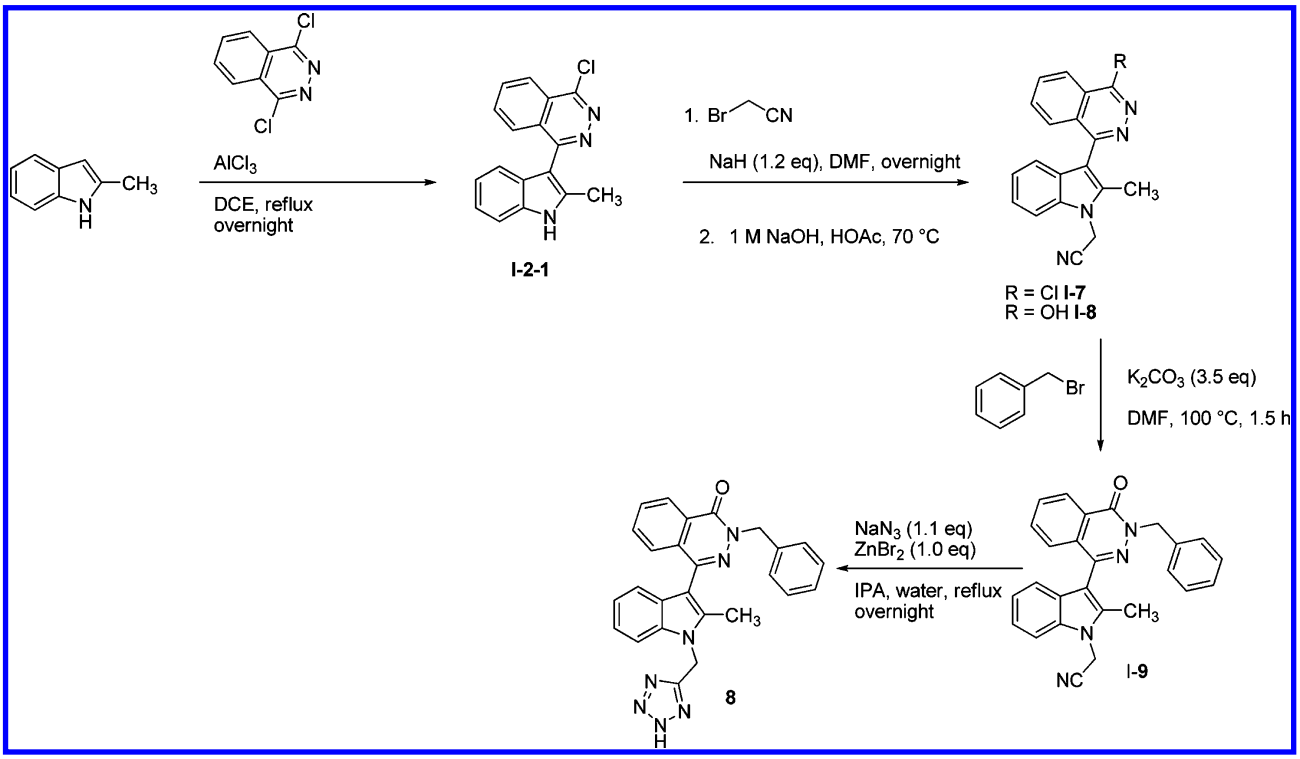

followed by deprotection yielding diazine indole acetic acids **2**–**26**, **28**, **29**, and **34**. The starting 2-methylindoles (**I-1**, Scheme 2) for some of the analogues required multistep synthesis. The 5-methylsulfonylindole (for preparation of **17**) was prepared by copper(I) catalyzed coupling reaction of **5**-bromoindole with sulfinic acid salt.[17] The synthesis strategy reported by Barluenga et al. was used to obtain 5,7-disubstituted indoles. The first step was selective ortho iodination of 2,4-disubstituted anilines. One of the following two iodinating agents was used: iodine in the presence of silver sulfate[18] or bis(pyridine)iodonium(I) tetrafluoroborate (IPy2BF4).[19] The second step was palladium-catalyzed coupling of the 2-iodoanilines with propyne, followed by copper iodide mediated nitrogen cyclization onto alkynes, resulting in 5,7-disubstituted indoles.[20]

The carboxylic acid modifications were studied on compound **3** (Scheme 3). Acid functionality was converted to

Scheme 5

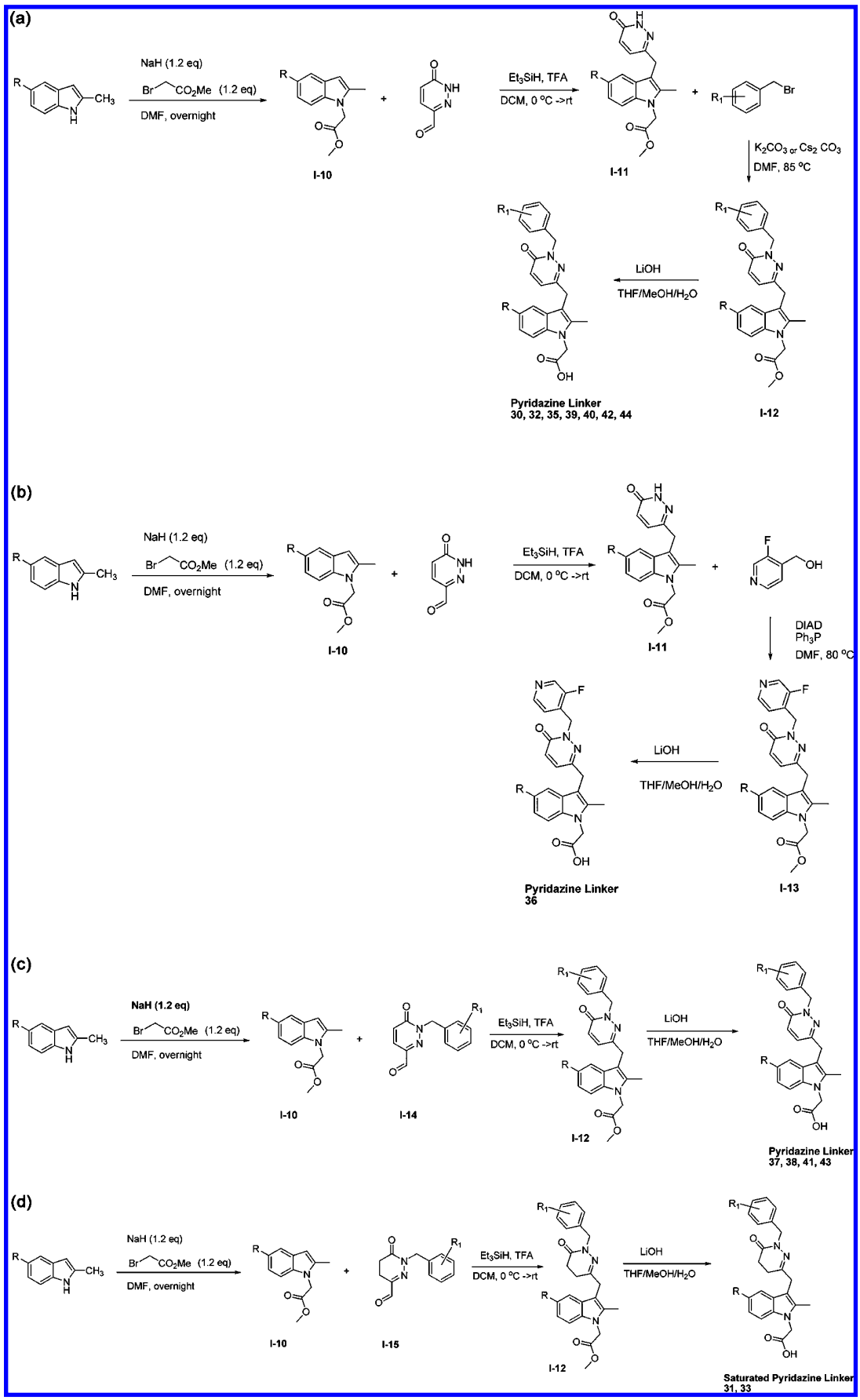
(a)
NaH (1.2 eq)
Br CO2Me (1.2 eq)
DMF, overnight
I-10
Et3SiH, TFA
DCM, 0 °C ->rt
I-11
K2CO3 or Cs2 CO3
DMF, 85 °C
LiOH
THF/MeOH/H2O
Pyridazine Linker
30, 32, 35, 39, 40, 42, 44
I-12
(b)
NaH (1.2 eq)
Br CO2Me (1.2 eq)
DMF, overnight
I-10
Et3SiH, TFA
DCM, 0 °C ->rt
I-11
DIAD
Ph3P
DMF, 80 °C
LiOH
THF/MeOH/H2O
Pyridazine Linker
36
I-13
(c)
NaH (1.2 eq)
Br CO2Me (1.2 eq)
DMF, overnight
I-10
I-14
Et3SiH, TFA
DCM, 0 °C ->rt
I-12
LiOH
THF/MeOH/H2O
Pyridazine Linker
37, 38, 41, 43
(d)
NaH (1.2 eq)
Br CO2Me (1.2 eq)
DMF, overnight
I-10
I-15
Et3SiH, TFA
DCM, 0 °C ->rt
I-12
LiOH
THF/MeOH/H2O
Saturated Pyridazine Linker
31, 33

Scheme 6

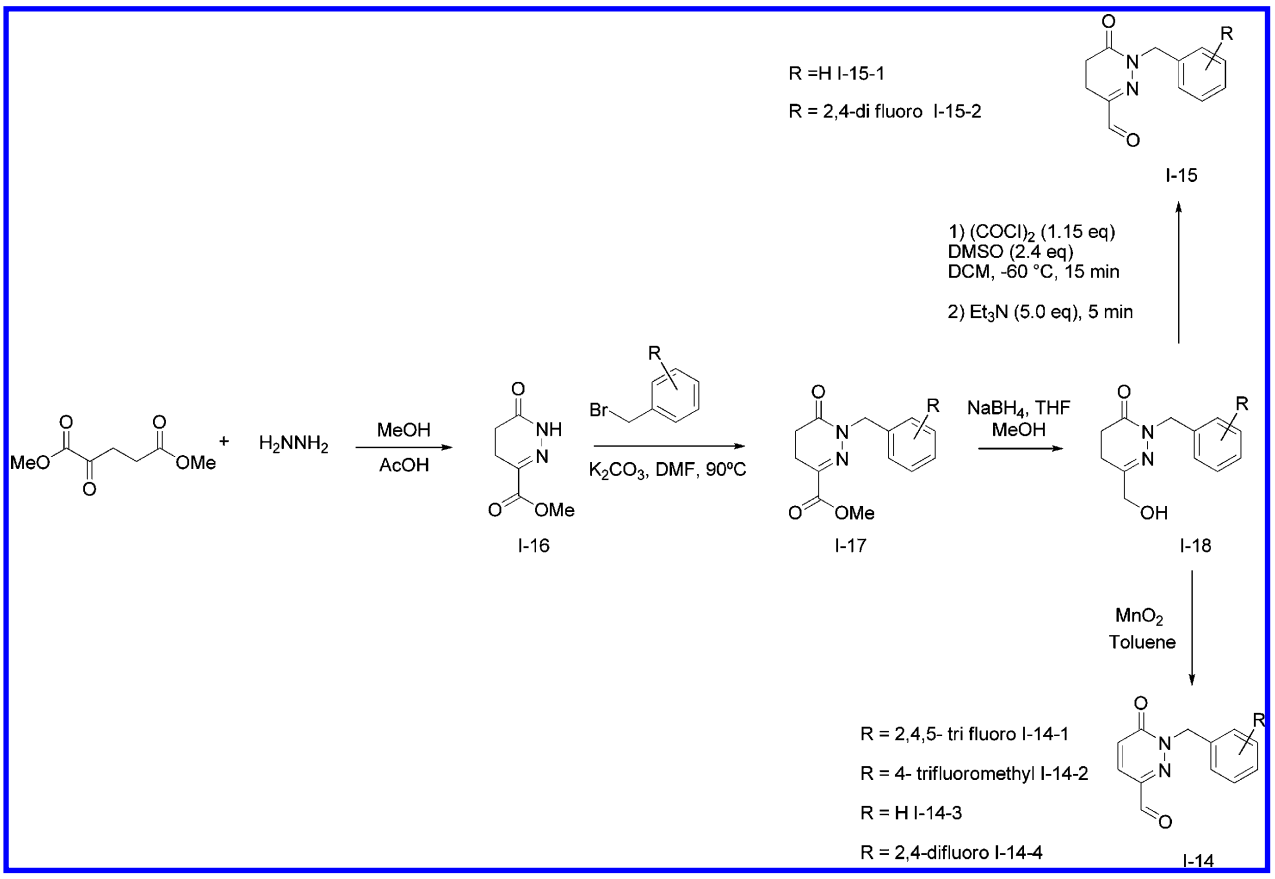

amides (**4**–**7**) via BOP mediated coupling. The carboxylic acid group in **3** was also converted to the corresponding alcohol (**9**) through mixed carbonic carboxylic acid anhydride formed in situ with ethyl chloroformate, followed by reduction with sodium borohydride. Tetrazole was also used as a surrogate for carboxylic acid. It was synthesized by addition of sodium azide to indole acetonitrile (**I-9**, Scheme 4) using zinc bromide as a catalyst.

The pyridazine linker compounds (**30**, **32**, **35**–**44**) were prepared by reductive alkylation of 2-methyl indoleacetate with 6-oxo-1,6-dihydropyridazine-3-carbaldehyde using triethyl silane/TFA mixture as the reducing agent (Scheme 5).[21] The resulting common intermediate **I-11** was derivatized in two ways: N-alkylation with various benzyl bromides using potassium or cesium carbonate (Scheme 5a) or Mitsonobu reaction with substituted benzyl alcohol (Scheme 5b). Since 6-oxo-1,6-dihydropyridazine-3-carbaldehyde was not readily available[22] for some analogues, the N-substituted pyridazine carbaldehyde (**I-14**) was presynthesized and then coupled with 2-methyl indoleacetate (Scheme 5c). Intermediate **I-14** were prepared by the method described by Olsen et al.[23] (Scheme 6). Commercially available dimethyl 2-oxopentanedioate was converted to dihydropyridazinone **I-16** using hydrazine in presence of acid. The nitrogen was then alkylated with substituted benzyl bromide using potassium carbonate. Reduction of **I-17** using sodium borohydride in a refluxing mixture of THF and methanol gave the primary alcohol **I-18**. The yields in this reaction were very sensitive to the rate of addition of methanol to the refluxing mixture of sodium borohydride and **I-17** in THF. Also the scale-up efforts of this reaction resulted in low yields. Treatment of **I-18** with activated manganese(IV) oxide in refluxing toluene afforded a tandem reaction where the primary alcohol was first oxidized to the aldehyde followed by oxidative aromatization to give **I-14**.

The saturated pyridazine linker compounds (**31**, **33**) (Scheme 5d) were accessed by reaction of 2-methyl indoleacetate with *N*-benzyl-6-oxo-1,4,5,6-tetrahydropyridazine-3-carbaldehyde (**I-15**). Intermediate **I-15** could be prepared by Swern oxidation of **I-18** (Scheme 6). For **33** this step gave a mixture of **I-15** and **I-14**. The mixture of intermediates was taken to the next step and then purified as final products.

In order to introduce a linker between the indole and phthalazine ring, we started with 2-indoleacetylbenzoic acid (**I-21**) and built the phthalazine ring by treatment with hydrazine (Scheme 7). Reaction of the resulting phthalazinone (**I-22**) with benzyl bromide resulted in isolation of only one product, the 2′-*N*-benzyl **I-23**. Next the indole nitrogen was alkylated with methyl bromoacetate followed by deprotection to give compound **27**.

■ RESULTS AND DISCUSSION

Preliminary SAR focused on optimization of substitution on the 5-position of indole and 3-position of the diazine in our initial lead **1**.[2] This effort led to the identification of **2**, which had lower molecular weight and clogP and overall improved lipophillic efficiency compared to **1**. In addition the replacement of the metabolically labile phenoxyethyl group in **1** with benzyl resulted in improved microsomal stability (Table 1, Figure 1). However, additional analogues were needed, as the new lead **2** had poor bioavailability in mouse. Further investigation showed **2** had low clearance but poor oral

Scheme 7

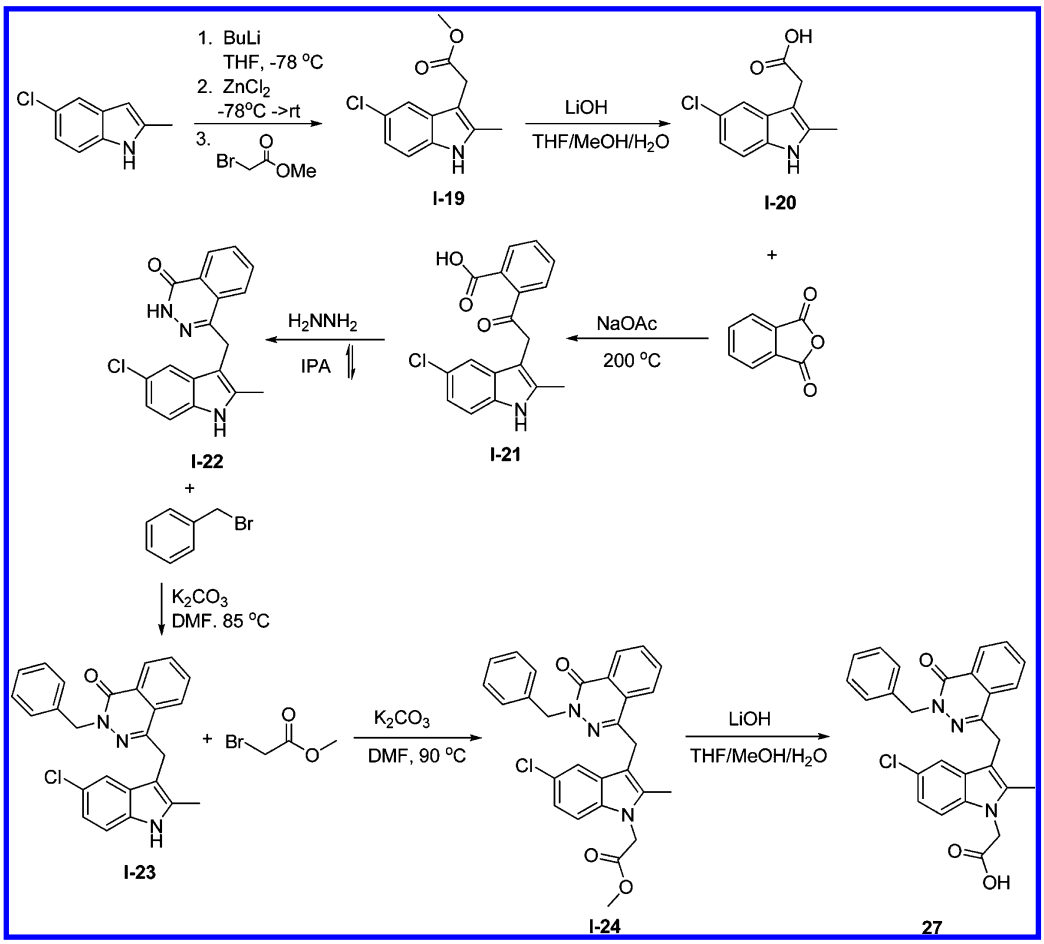

Table 1. Comparative Profiles for Compounds 1 and 2

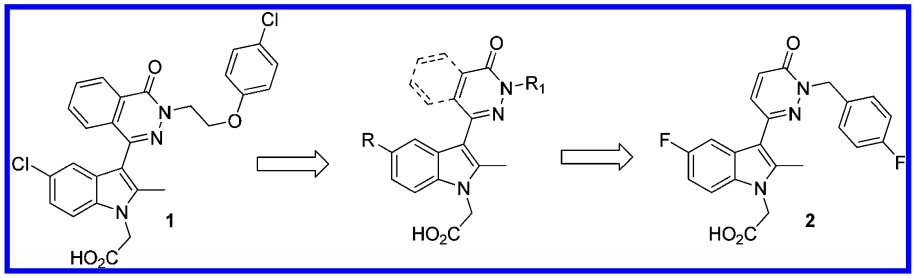

compd	MW	clogP	hCRTH2 FRET IC_{50} (nM)	mouse PK Cl (mL min^{-1} kg^{-1})	F (%)	microsomal stability mouse, $t_{1/2}$ (min)	Caco-2 permeability, $P_e \times 10^{-6}$ (cm/s)
1	522	5.9	2	>90	<1	11	0.2
2	4.9	3.5	20	6.9	11	>30	0.3

exposure. The in vitro ADME profile of **2** showed good microsomal stability toward oxidative metabolism in mouse and human liver microsomes but poor permeability in the Caco-2 cell assay, as expected for a lipophilic and zwitterionic carboxylic acids. Since the carboxylic acid functionality is part of the pharmacophore, we tried to find a replacement. Table 2 shows some of our efforts toward this. Replacing the carboxylic acid with tetrazole (**8**) was deleterious to CRTH2 activity. Conversion of the acid to amide (**4**), substituted amide (**5** and **6**), and aliphatic sulfonamide (**7**) all resulted in loss of potency. Likewise, addition of a methyl group at the methylene next to the carboxylic acid reduced potency (**10**). The length of the spacer between the indole and carboxylic acid was found to be of crucial importance; a two-carbon chain (**11**) led to complete loss of potency. Further structural changes were made to vary the clogP and pK_a of the carboxylic acid, which can modulate the permeability of these compounds. First, the potency of the new analogues was measured to determine what structural variation could be tolerated. At first the substitution on the A ring of indole was studied (Table 3). Substituents at the 5-position had an important effect on activity. Hydrophobic groups (entries **13**−**16**) were preferred, and polar groups (entries **17**, **18**, **25**) had a detrimental effect on potency. Substitution at the 7-position reduced activity (entries **19**−**25**). The size of the substituent at the 7-position was also important; larger substituents showed the worst activity (**14** vs **20** vs **21**

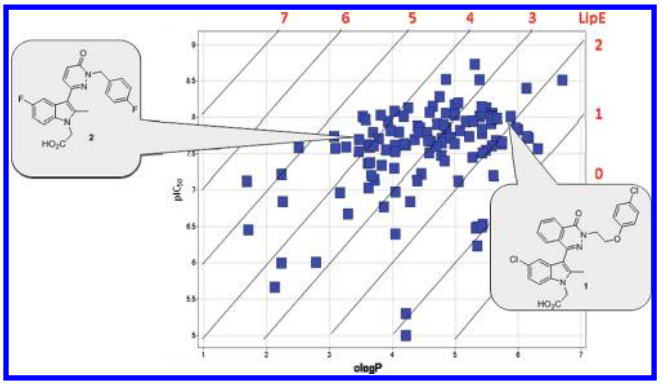

Figure 1. Identification of leads with improved lipophillic efficiency: plot of hCRTH2 FRET (IC_{50}) and clogP.

Table 2. Carboxylic Acid Replacement

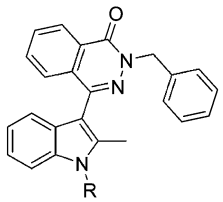

Compound	3	4 - 11
hCRTH2 FRET IC_{50}	0.016 uM	>1 uM

Compound	R
3	CH_2CO_2H
4	CH_2CONH_2
5	$CH_2CON(Me)_2$
6	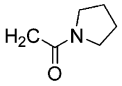
7	$CH_2CONHSO_2Me$
8	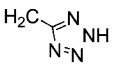
9	CH_2CH_2OH
10	$CH(Me)CO_2H$
11	$CH_2CH_2CO_2H$

and **15** vs **22** vs **23** vs **24**). None of the new analogues showed good potency.

Next, addition of a methylene linker between the pyridazine and indole was investigated. An in-house passive permeability model[24] was used to calculate the permeability of benzylpyridazineindoles with and without linker. Figure 2a shows that linker-containing compounds are predicted to have improved apparent permeability (P_{app}) and the higher the faster the compound crosses the cell monolayer. Several linker-containing analogues were therefore prepared and first evaluated in the FRET assay. The pyridazine linker compounds were somewhat more potent than the pyridazines (Figure 2b). Addition of a linker in the phthalazine series maintained potency (for example, **26** vs **27**, Table 4). The phthalazine linker compounds were not pursued because of high molecular weight and clogP. Another approach to increase permeability could be via improvement of solubility. We hypothesized that reduction of the diazine ring would disrupt planarity of the indole−diazine system, resulting in improved solubility. A 10-fold loss in potency was seen for the saturated phthalazinones (**28** vs **29**, Table 4). However, in the linker series saturated compounds maintained potency (**30** vs **31** and **32** vs **33**, Table 4). This SAR study led to identification of the diazine linker series which was found to be comparable to or a bit more potent than the pyridazines.

Table 3. SAR of Substitution on the Indole Ring

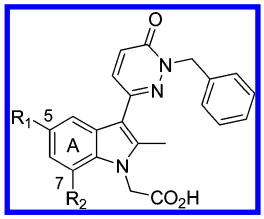

compd	R_1	R_2	hCRTH$_2$ FRET IC_{50} (μM)	clogP	pK_a
12	H	H	0.134	3.17	4.15
13	Br	H	0.016	4.05	4.03
14	Cl	H	0.028	3.90	4.03
15	F	H	0.023	3.33	4.02
16	Me	H	0.034	3.17	4.16
17	$MeSO_2$	H	0.135	1.71	4.00
18	OMe	H	0.104	3.21	4.07
19	H	Br	>2	1.05	3.98
20	Cl	F	0.090	1.05	3.86
21	Cl	Cl	1.69	1.62	3.88
22	F	F	0.076	3.48	3.85
23	F	Cl	0.245	4.05	3.86
24	F	$MeSO_2$	>1	1.91	3.83
25	$MeSO_2$	F	0.934	1.91	3.83

Next, the permeability of these compounds was measured in the Caco-2 cell line at reduced pH 6.5 to minimize the effect that the carboxylic acid moiety may have on overall permeability. Table 5 shows the effect of the linker on permeability. The pyridazine linker compounds exhibited acceptable permeability across Caco-2 monolayers, suggesting that the brush-border (microvilli) region of the jejunum segment of the small intestine (where the pH is slightly acidic) may be a predominant site of absorption. The permeability data for these compounds suggest that absorption and bioavailability (after oral administration) should not be limited by permeability. Compounds **2** and **4** showed 3-fold improvement in oral exposure in mouse, confirming our original hypothesis that poor oral exposure was due to poor permeability. A similar trend was seen for rat PK. Figure 3 shows a plot of oral exposure in rat and permeability for some of the pyridazines and linker-pyridazine. It is clear that the linker-pyridazine compounds have higher permeability and oral exposure compared to the pyridazines. Representative examples in the pyridazine linker series exhibited good potency, permeability, and PK. On the basis of these observations, this series was prioritized for further creation of analogues.

For confirmation of potency, compounds potent in the FRET assay were also tested in a secondary assay. CRTH2 mediated cell migration by our inihibitors was examined in a basophil chemotaxis assay. This assay was run in a 96-transwell format with human CRTH2+ basophils, derived from IL-3 treated CD34+ progenitor cells, in the presence of 10 nM PGD2. An initial set of compounds were tested in the chemotaxis assay, and a very good correlation was observed between the FRET and chemotaxis assays (Figure 4a). Representative examples were also tested in a hCRTH2 competitive binding assay with tritium labeled PGD2. A good correlation was observed between binding assay and the FRET assay, confirming that the FRET potency was coming from direct binding to hCRTH2 (Figure 4b). Since a good correlation (within 10-fold) was established between the FRET and chemotaxis and between FRET and binding assays, only advanced compounds were tested in these assays.

Ligands for the receptors in the prostaglandin family show some degree of cross-reactivity, and there is potential for small molecule inhibitors to do the same. Therefore, selectivity of

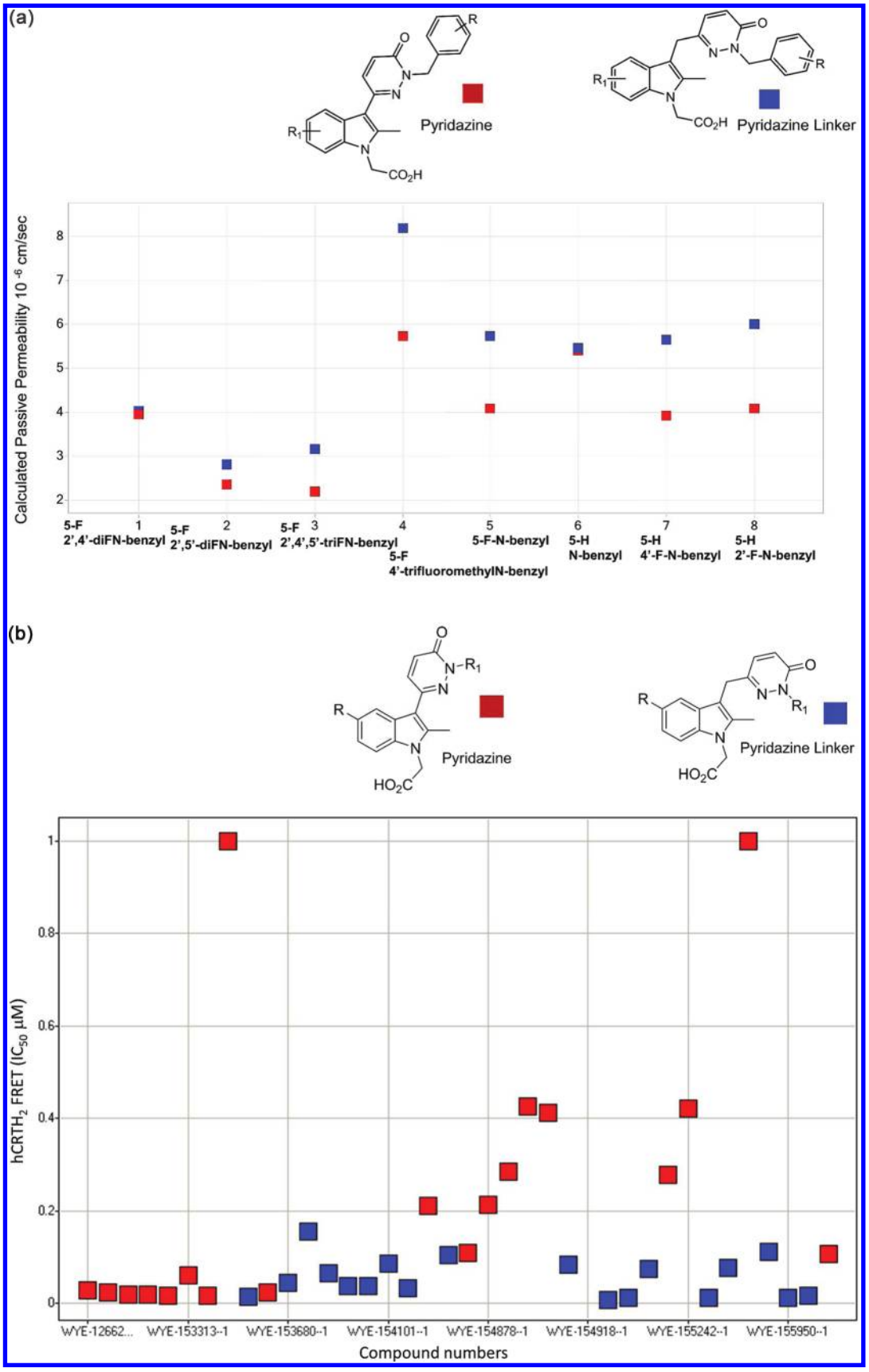

Figure 2. Comparison of calculated permeability (a) and hCRTH2 potency (b) between pyridazine and pyridazine linker series.

these compounds against two other prostaglandin receptors (DP1 and TXB2) was investigated. For DP1 a cAMP TR-FRET assay in endogenously expressing NK-92 cells was used. For TXB2, a receptor binding assay was established.

Table 4. Antagonist Activity of Saturated Diazines against hCRTH2 in FRET Assay

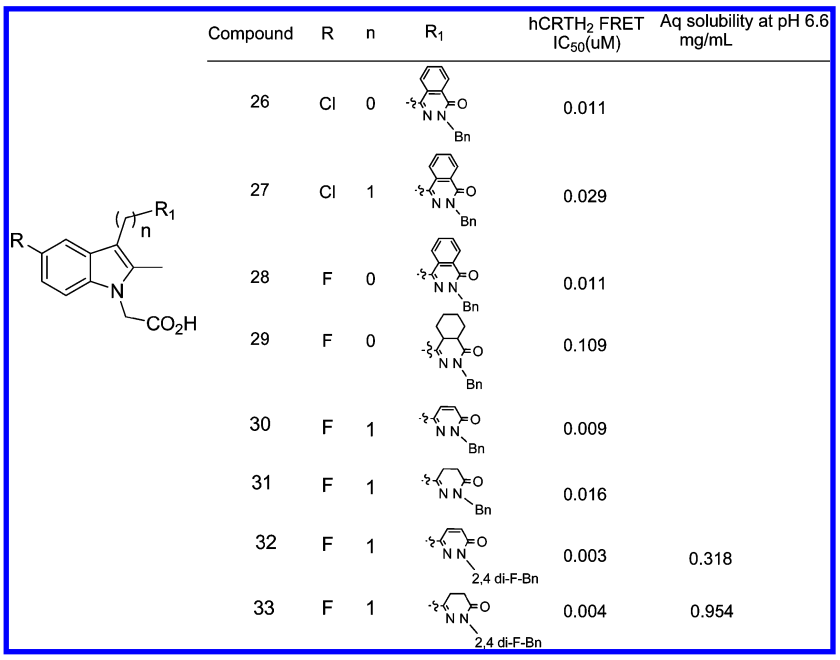

Compound	R	n	R_1	hCRTH$_2$ FRET IC$_{50}$(uM)	Aq solubility at pH 6.6 mg/mL
26	Cl	0	Bn	0.011	
27	Cl	1	Bn	0.029	
28	F	0	Bn	0.011	
29	F	0	Bn	0.109	
30	F	1	Bn	0.009	
31	F	1	Bn	0.016	
32	F	1	2,4 di-F-Bn	0.003	0.318
33	F	1	2,4 di-F-Bn	0.004	0.954

Table 5. Comparison of Caco-2 Permeability of Pyridazine and Linker Containing Compounds 30 and 32 Compared to 15 and 34, Respectively[a]

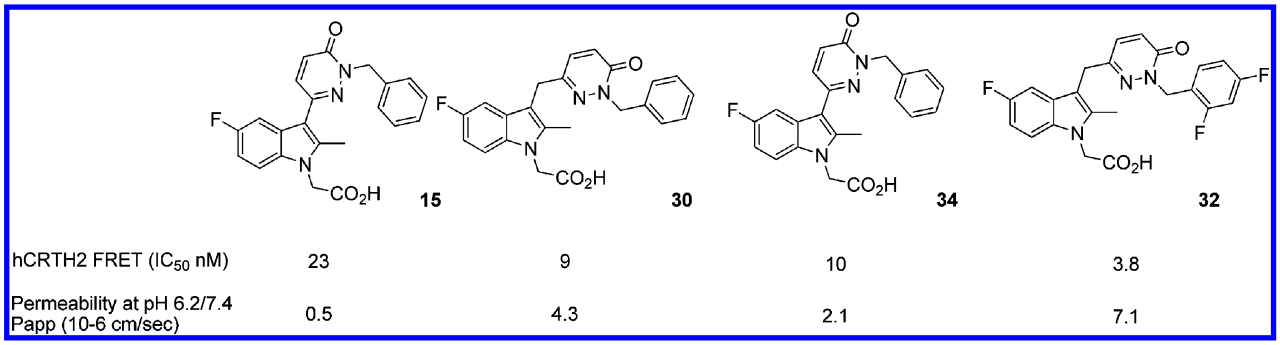

	15	30	34	32
hCRTH2 FRET (IC$_{50}$ nM)	23	9	10	3.8
Permeability at pH 6.2/7.4 Papp (10-6 cm/sec)	0.5	4.3	2.1	7.1

[a]Mouse PK studies showed 3-fold improvements in po exposure for compounds **30** and **32** compared to **15** and **34**, respectively.

Representative examples from the series were tested and found to be greater than 1000-fold selective against CRTH2. Early compounds were also tested for affinity to the mouse CRTH2 receptor. A good correlation was seen between the human and murine CRTH2. This result is of importance for the feasibility of in vivo pharmacological studies in mouse models. Compounds were tested in these assays before advancing to in vivo models.

Additionally, a human whole blood eosinophil shape change assay (hEOS) was developed. Eosinophil shape change is a consequence of cytoskeleton reorganization predisposing the leukocyte for cell movement and transmigration and can be quantified by flow cytometry through changes in forward light scatter. In this assay human whole blood was stimulated with PGD2 and analyzed by flow cytometry. Eosinophils were selected based on their autofluorescence in the FL2 channel. Shape change was estimated based on mean forward light scatter values. This assay could potentially be used as a biomarker in in vivo models and clinical trials. Potency in the FRET assay ($IC_{50} \geq 50$ nM) and good chemical properties were used as filters to advance compounds to the hEOS assay. The earlier diazines did not show a correlation between the FRET and whole blood data. However, the later diazine linker series showed a good correlation between the two assays with a drop-off of less than 10-fold (Table 6). In general these compounds have high plasma protein binding (>98%) (for example, compound **32** in an equilibrium dialysis experiment had a free fraction of 2% in human plasma). Eight compounds from Table 6 were selected for in vivo evaluation. Compounds were selected based on permeability, hEOS, and structure (diversity and structural alerts).

■ IN VIVO STUDIES

We have utilized an oxazolone induced contact hypersensitivity (CHS) model in the mouse as a primary in vivo screen. In this model mice are sensitized with oxazolone on their shaved abdomen and then challenged on day 5 by painting their ears with oxazolone. On the day of challenge the test compound is administered and inhibition of ear swelling is determined as a measure of efficacy. A 50−60% reduction in ear swelling was observed with CRTH2 knockout mice. Selected compounds were tested in this model at 3 mg/kg po b.i.d. Figure 5a shows results for analogues from the pyridazine linker series. The data suggest that the compounds need to be very potent ($IC_{50} < 5$ nM) in the hEOS assay to be efficacious in the CHS model.

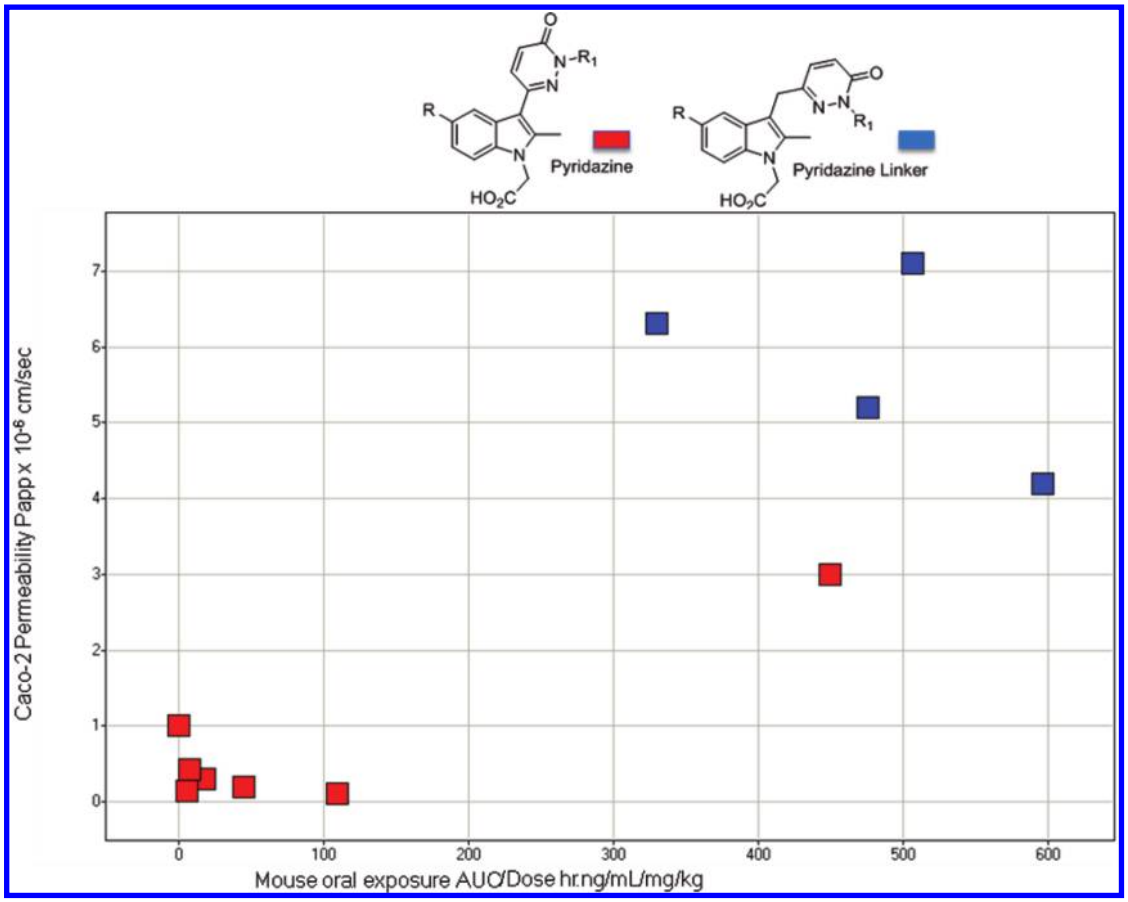

Figure 3. Plot of permeability and oral exposure in mouse for the pyridiazine linker analogues.

Two compounds, **32** and **31**, showed 30% and 34% reduction in ear swelling in the oxazolone CHS model at 3 mg/kg po b.i.d., respectively. Both compounds showed moderate Caco-2 permeability and were progressed into in vivo rat pharmacokinetic studies. The compounds had low to moderate clearance and good in vivo exposure and bioavailability (Table 7). However, **32** was taken forward because of overall better profile. A dose response study for **32** in the CHS model gave a MED of 1 mg/kg (Figure 5b).

Next, we sought to evaluate the potential of compound **32** to modulate house dust mite (HDM) induced allergic airway disease in mice (Figure 6). HDM is a natural airborne allergen that can trigger asthma attacks in susceptible patients. Similar to asthmatics, mice repeatedly challenged intratracheally with HDM develop allergic airway disease with prominent eosinophilia.[25] When dexamethasone (Dex) was injected intraperitoneally at 1 mg/kg (q.d.), airway inflammation was almost completely abrogated. The total number of inflammatory cells in bronchoalveolar lavage (BAL) samples and BAL eosinophilia macrophage and lymphocyte numbers were decreased to baseline levels. The number of neutrophils was seemingly decreased as well, albeit below statistical significance; however, it is worth noting that neutrophils represent the smallest cell population found in BAL samples in this model. When compound **32** was administered orally at 20 mg/kg (q.d.), airway inflammation was also largely alleviated. Total BAL cellularity, BAL eosinophilia, and BAL lymphocyte numbers were significantly reduced. Conversely, BAL macrophage numbers did not significantly change while the subjective decrease of neutrophil numbers remained below statistical significance. The microscopic examination of H&E-stained lung tissue sections from control and treated animals showed that HDM challenge resulted in bronchovascular and alveolar inflammation dominated by lymphocytic and histiocytic infiltrates, with fewer neutrophils and occasional eosinophils. HDM challenge also resulted in increased intraepithelial mucus formation along with epithelial/endothelial hyperplasia and hypertrophy. Treatment with compound **32** substantially alleviated these pathological features, including the size of inflammatory infiltrates and the thickening of the respiratory epithelium and blood vessels.

To explore efficacy in a non-rodent species and to determine effects on lung function, **32** was evaluated in a sheep model of *Ascaris* induced airway bronchoconstriction and AHR (Figure 7a).[26] In this model sheep that are naturally sensitized to the nematode *Ascaris* are challenged via the airways to induce both an early phase allergic airway bronchoconstriction (EAR), late phase allergic airway bronchoconstriction (LAR), and AHR to aerosolized carbachol. Compound **32**, when dosed at 3 mg/kg iv b.i.d. the day prior to challenge and then again 1 h prior to challenge, completely blocked the LAR and attenuated the EAR by approximately 38%. The animals were also given a fourth dose of **32**, 8 h after challenge, to evaluate attenuation of AHR to aerosolized carbachol that was measured the day following allergen challenge. By use of this dosing regimen, **32** (3 mg/kg iv) completely blocked the allergen induced AHR to carbachol. Conversely, **32** was not efficacious when administered at 1 mg/kg iv in an identical dosing regimen. **32** was also evaluated for efficacy following subchronic administration at 1 mg/kg iv q.d. for 7 days prior to challenge. In this dosing regimen, the

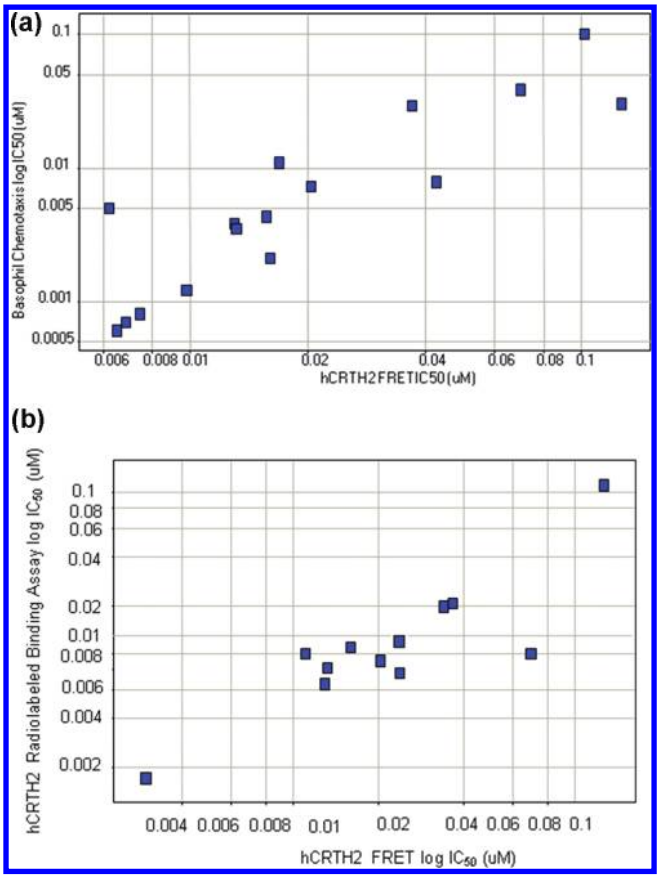

Figure 4. (a) Plot of log(IC_{50}) in the FRET and basophil chemotaxis assay. (b) Plot of log(IC_{50}) in the FRET and binding assay.

compound completely blocked the LAR and AHR. Interestingly, similar to the results observed at 3 mg/kg, **32** also attenuated the EAR (by approximately 20%). Following measurement of AHR, three bronchi from each sheep were lavaged and cell counts determined. **32** reduced BAL inflammation at this dose (Figure 7b).

Preliminary studies also point to a role for CRTH2 in impaired airway mucociliary clearance after allergen challenge. Tracheal mucus velocity (TMV), a marker of airway mucociliary clearance, is measured in sheep by a technique in which radiopaque disks are insufflated into the trachea (Figure 7c). The cephalad-axial velocities of the individual disks are then recorded and calculated. Following allergen challenge the TMV of the beads was reduced to approximately 50% of baseline TMV at 4 h after challenge; TMV remained attenuated for up to 24 h after allergen challenge. Administration of **32** at 3 mg/kg iv resulted in a more rapid return to baseline levels with a TMV of approximately 70% of baseline at 4 h and a TMV of 98% of baseline at 8 h compared to an 8 h TMV of 47% of baseline with vehicle treated animals. Five sheep were used for these studies.

Compound **32** was further profiled in safety and selectivity studies (Table 8). On the basis of CYP inhibition data, there were no drug–drug interaction concerns (tested against six isoforms 3A4, 2D6, 2C9, 2C19, 2C8, 2B6, 1A2, 2A6, with IC_{50} ranging from 16 to 100 uM). The compound was clean in the AMES assay. No hERG inhibition was seen at 33 μM. Greater than 500-fold selectivity was seen against DP1 and TP receptors and in the Novascreen and nuclear receptor panel. On the basis of these results and in vivo efficacy, **32** (CRA-898) was advanced to development track.

■ CONCLUSION

We have discovered a new class of CRTH2 antagonists, the pyridazine linker containing indole acetic acids. The initial hit **1** had good potency but poor permeability, metabolic stability, and PK. Careful design and optimization of physicochemical properties afforded a series with good potency, low rate of metabolism, moderate permeability, and good oral bioavailability in rodents. **32** was identified as the development track candidate. It is potent in cell based, binding, and whole blood assays. **32** exhibits low clearance and good exposure in mouse and rat. It was efficacious in a mouse model of contact hypersensitivity with an MED of 1 mg/kg b.i.d. When administered perorally at 20 mg/kg (q.d.), it alleviated airway inflammation in the HDM model. In a sheep model of *Ascaris* induced allergic airway bronchoconstriction, inflammation, and AHR, a subchronic administration at 1 mg/kg iv completely blocked the LAR and AHR and attenuated the EAR phase.

■ EXPERIMENTAL SECTION

Chemistry. Reactions were run using commercially available starting materials and solvents, without further purification. Proton NMR spectra were recorded at 300 MHz on a Varian Gemini 2000 or at 400 MHz on a Bruker AV-400 spectrometer using TMS (δ 0.0) as a reference. Combustion analyses were obtained using a Perkin-Elmer series II 2400 CHNS/O analyzer. CHN analyses were carried out by Robertson-Microlit. Where analyses are indicated by symbols of the elements, analytical results obtained for those elements were within 0.4 of the theoretical values. Low resolution mass spectra were obtained using a Micromass platform electrospray ionization quadrupole mass spectrometer. High resolution mass spectra were obtained using a Bruker APEXIII Fourier transform ion cyclotron resonance (FT-ICR) mass spectrometer equipped with an actively shielded 7 T superconducting magnet (Magnex Scientific, Ltd., U.K.) and an external Bruker APOLLO electrospray ionization (ESI) source. The microwave procedures were carried out with a Biotage microwave. Preparative HPLC was run using a Waters reverse phase preparative HPLC instrument with an Xterra C18 5 μm, 30 mm × 100 mm column. The flow rate was 40 mL/min. Mobile phase A was water. Mobile phase B was acetonitrile, and triethylamine was used as a modifier. Purity in two solvent systems [water–acetonitrile (method 1) and water–methanol (method 2)] was determined using an Agilent 1100 HPLC instrument, and all compounds analyzed were >95% pure. The indoles used were either commercially available or prepared by general procedure B.

General Procedure A (Scheme 1). Intermediate I-1b. In a two-necked 500 mL round-bottomed flask, under nitrogen, 2-methylindole (5.00 g, 38.1 mmol) was taken up in 100 mL of anhydrous DMF. Sodium hydride (1.83 g of a 60 wt % mineral oil suspension, 1.10 g, 45.7 mmol) was added and the reaction mixture stirred for 30 min. Appropriate bromide (46 mmol) was then added by syringe, and the mixture was stirred overnight. It was then quenched with 10 mL of saturated ammonium chloride solution and partitioned between 400 mL each of ethyl acetate and brine. The aqueous layer was extracted with an additional 100 mL of ethyl acetate. The combined organic extracts were washed with brine (3×), dried over $MgSO_4$, filtered, and evaporated. The crude product was purified by flash chromatography over silica gel

Intermediate I-2. In a 500 mL round-bottomed flask, the appropriate indole (**I-1a** or **I-1b**, 6.04 mmol) and 1,4-dichlorophthalazine or 3,6-dichloropyridazine (6.34 mmol) were taken up in 80 mL of dichloroethane. Aluminum chloride (8.46 mmol) was added, and the mixture was refluxed overnight under a nitrogen-filled balloon. In some cases the mixture was stirred in the microwave at 160 °C for 1 h. After cooling slightly, the reaction mixture was poured into a

Table 6. Inhibition of Human Eosinophil Shape Change Induced by PGD2

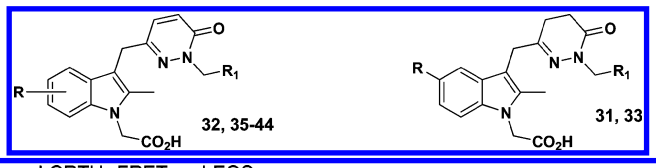

Compound	R	R_1	hCRTH$_2$ FRET (IC_{50} nM)	hEOS (IC_{50} nM)	Compound	R	R_1	hCRTH$_2$ FRET (IC_{50} nM)	hEOS (IC_{50} nM)
32	5-F	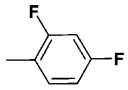	3	3	**41**	5-F	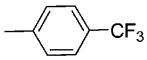	16	55
35	5-F	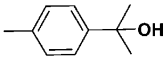	5	13	**42**	5-F	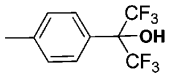	7	57
36	5-F		6	6	**43**	H		32	155
37	5-F	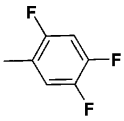	0.8	10	**44**	5,7-diF	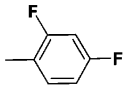	28	180
38	5-Cl		15	15	**31**	F		1.5	4
39	H	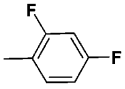	20	20	**33**	F	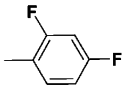	4	8
40	5-F	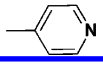	12	22					

mixture of ice and 2 M hydrochloric acid. This was stirred until all the ice had melted, and the layers were separated. The aqueous layer was extracted with additional dichloroethane, and the combined organic extracts were washed with brine, dried over anhydrous magnesium sulfate, filtered, and evaporated to give material of sufficient purity to be used directly in the next step.

Intermediate I-3. **I-2** (5.94 mmol), potassium carbonate (11.9 mmol), and bromoacetate (12 mmol) were taken up in 30 mL of DMF in a 250 mL round-bottomed flask and heated at 70 °C overnight. The reaction mixture was then poured into water, extracted into ethyl acetate (3×), washed with brine (3×), dried over anhydrous magnesium sulfate, filtered, and evaporated. The crude product was purified by flash chromatography over silica gel to give pure product.

Intermediate I-4. In a round-bottomed flask, **I-3** was taken up in 100 mL of acetic acid, and 20 mL of 1 M sodium hydroxide was added. The mixture was heated at 70 °C for 1 h until LC−MS analysis indicated complete conversion to product. It was then partitioned between 175 mL each of ethyl acetate and brine, and the aqueous layer was extracted with additional ethyl acetate. The combined organic extracts were washed with water (3×) and brine, dried over anhydrous magnesium sulfate, filtered, evaporated, and azeotroped with toluene to give pure product

Diazine Indole Acetic Acid. **I-4** (0.548 mmol), potassium carbonate (1.92 mmol), and appropriate benzyl bromide (1.64 mmol) were taken up in 8 mL of DMF and heated at 85 °C for 2.5 h until LC−MS analysis showed complete consumption of starting material. The mixture was then cooled to room temperature, poured into 80 mL of water, extracted into ethyl acetate, washed with brine, dried over anhydrous magnesium sulfate, filtered, and evaporated. For the *tert*-butyl ester containing compounds, trifluoroacetic acid was added to the crude ester, and this reaction mixture was stirred for 1 h, until LC−MS analysis showed complete disappearance of the ester. The mixture was then evaporated and purified by flash chromatography over silica gel. For the methyl/ethyl ester containing compounds the crude ester was taken up in 3:1 ratio of methanol:/tetrahydrofuran, and a solution of lithium hydroxide (2 equiv) in water was added. After the mixture was stirred for 2 h at room temperature, LC−MS analysis showed complete consumption of starting material. The reaction mixture was evaporated and purified by flash chromatography over silica gel.

2-(5-Fluoro-3-(3-(4-fluorobenzyl)-4-oxo-3,4-dihydrophthalazin-1-yl)-2-methyl-1*H*-indol-1-yl)acetic Acid (2). Y = Me. Solid (overall yield, 7%). ^{1}H NMR (400 MHz, DMSO-d_6) δ 13.29 (br s, 1 H), 7.75 (d, J = 9.6 Hz, 1 H), 7.40−7.51 (m, 3 H), 7.30 (dd, J = 10.1, 2.5 Hz, 1 H), 7.16−7.23 (m, 2 H), 7.05 (d, J = 9.6 Hz, 1 H), 6.98 (td, J = 9.2, 2.4 Hz, 1 H), 5.33 (s, 2 H), 5.01 (s, 2 H), 2.41 (s, 3 H). HRMS: calcd for $C_{22}H_{17}F_2N_3O_3$ + H$^+$, 410.131 07; found (ESI, [M + H]$^+$ obsd), 410.1305.

2-(3-(3-Benzyl-4-oxo-3,4-dihydrophthalazin-1-yl)-2-methyl-1*H*-indol-1-yl)acetic Acid (3). Y = *t*-Bu. Solid (overall yield, 23%). ^{1}H NMR (DMSO-d_6) δ: 13.14 (br s, 1H), 8.37−8.43 (m, 1H), 7.82−7.93 (m, 2H), 7.53−7.58 (m, 1H), 7.48−7.53 (m, 1H), 7.32−7.41 (m, 4H), 7.26−7.32 (m, 1H), 7.11−7.19 (m, 2H), 6.99 (ddd, J = 8.0, 7.0, 0.9 Hz, 1H), 5.35−5.50 (m, 2H), 5.10 (s, 2H), 2.23 (s, 3H). HRMS (ESI+) calcd for $C_{26}H_{21}N_3O_3$ (MH$^+$) 424.1653; found 424.1656

2-(3-(3-Benzyl-4-oxo-3,4-dihydrophthalazin-1-yl)-2-methyl-1*H*-indol-1-yl)propanoic Acid (10). Y = Me. Solid (overall yield, 95.2%). ^{1}H NMR (400 MHz, DMSO-d_6) δ 8.37−8.43 (m, 1H), 7.80−7.93 (m, 2H), 7.49−7.59 (m, 1H), 7.25−7.44 (m, 6H), 7.08−7.16 (m, 2H), 6.94−7.01 (m, 1H), 5.34−5.54 (m, 3H), 2.28 (s, 3H), 1.69 (dd, J = 6.32, 7.07 Hz, 3H). HRMS: calcd for $C_{27}H_{24}N_3O_3$ + H$^+$, 438.1812; found (ESI, [M + H]$^+$ obsd), 438.1816.

3-(3-(3-Benzyl-4-oxo-3,4-dihydrophthalazin-1-yl)-2-methyl-1*H*-indol-1-yl)propanoic Acid (11). Y = Me. Solid (overall yield, 69%). ^{1}H NMR (400 MHz, DMSO-d_6) δ 12.46 (s, 1H), 8.37−8.41 (m, 1H), 7.80−7.92 (m, 2H), 7.53−7.59 (m, 2H), 7.26−7.40 (m, 5H),

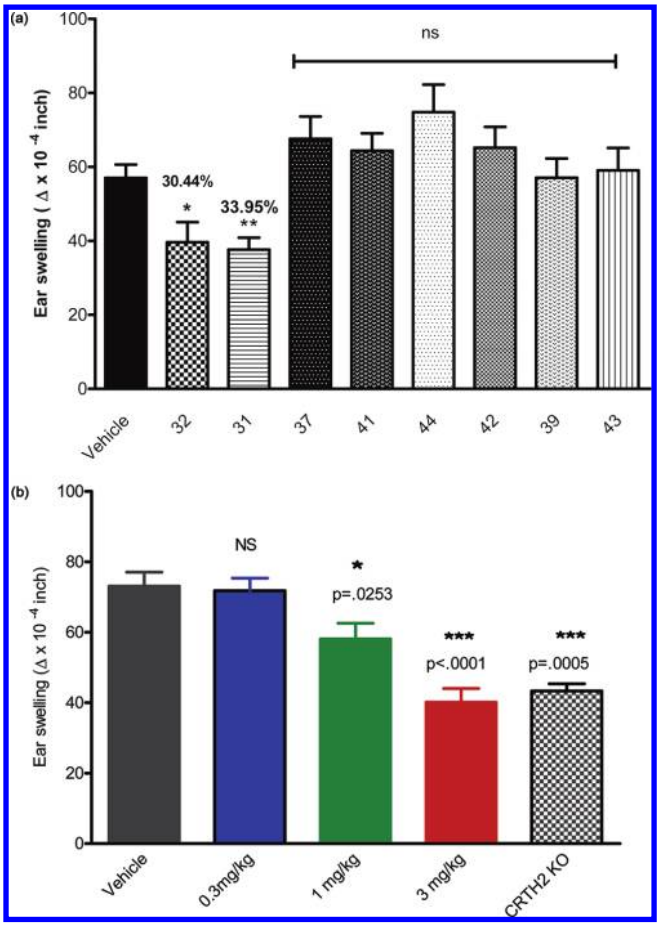

Figure 5. (a) In vivo efficacy in CHS model. (b) MED for compound **32** in CHS model.

7.10−7.19 (m, 2H), 6.98 (ddd, J = 1.01, 7.01, 7.89 Hz, 1H), 5.34−5.48 (m, 2H), 4.47 (t, J = 7.33 Hz, 2H), 2.77 (t, J = 7.20 Hz, 2H), 2.33 (s, 3H). HRMS: calcd for $C_{27}H_{24}N_3O_3 + H^+$, 438.1812; found (ESI, $[M + H]^+$ obsd), 438.1819

2-(3-(1-Benzyl-6-oxo-1,6-dihydropyridazin-3-yl)-2-methyl-1*H*-indol-1-yl)acetic Acid (12). Y = Me. Solid (overall yield, 26.9%). ^{1}H NMR (400 MHz, DMSO-d_6) δ 13.16 (br s, 1 H), 7.76 (d, J = 9.6 Hz, 1 H), 7.62 (d, J = 7.8 Hz, 1 H), 7.46 (d, J = 8.1 Hz, 1 H), 7.28−7.39 (m, 5 H), 7.12−7.18 (m, 1 H), 7.03−7.09 (m, 2 H), 5.34 (s, 2 H), 5.05 (s, 2 H), 2.41 (s, 3 H). HRMS: calcd for $C_{22}H_{19}N_3O_3 + H^+$, 374.149 92; found (ESI, $[M + H]^+$ obsd), 374.1498.

2-(3-(1-Benzyl-6-oxo-1,6-dihydropyridazin-3-yl)-5-bromo-2-methyl-1*H*-indol-1-yl)acetic Acid (13). Y = Me. Solid (overall yield, 48%). ^{1}H NMR (400 MHz, MeOD) δ ppm 2.31 (s, 3 H), 4.83 (s, 2 H), 5.30 (s, 2 H), 6.95 (d, J = 9.60 Hz, 1 H), 7.17−7.24 (m, 2 H), 7.24−7.31 (m, 3 H), 7.37 (d, J = 8.34 Hz, 2 H), 7.58 (d, J = 9.60 Hz, 1 H), 7.65−7.69 (m, 1 H). HRMS calcd for ($C_{22}H_{18}BrN_3O_3 + H^+$), 452.0604; found, 452.0603.

2-(3-(1-Benzyl-6-oxo-1,6-dihydropyridazin-3-yl)-5-chloro-2-methyl-1*H*-indol-1-yl)acetic Acid (14). Solid (overall yield, 50%). Y = Me. ^{1}H NMR (400 MHz, DMSO-d_6) δ ppm 2.42 (s, 3 H), 5.08 (s, 2 H), 5.35 (s, 2 H), 7.06 (d, J = 9.60 Hz, 1 H), 7.16 (dd, J = 8.60, 2.02 Hz, 1 H), 7.27−7.42 (m, 5 H), 7.51 (d, J = 8.84 Hz, 1 H), 7.57−7.65 (d, J = 2.02 Hz, 1 H), 7.76 (d, J = 9.60 Hz, 1 H).

2-(3-(1-Benzyl-6-oxo-1,6-dihydropyridazin-3-yl)-5-fluoro-2-methyl-1*H*-indol-1-yl)acetic Acid (15). Y = Me. Solid (overall yield, 17.4%). ^{1}H NMR (400 MHz, DMSO-d_6) δ 13.17 (br s, 1 H), 7.75 (d, J = 9.9 Hz, 1 H), 7.49 (dd, J = 8.8, 4.5 Hz, 1 H), 7.27−7.41 (m, 6 H), 7.06 (d, J = 9.6 Hz, 1 H), 6.99 (td, J = 9.2, 2.7 Hz, 1 H), 5.35 (s, 2 H), 5.07 (s, 2 H), 2.41 (s, 3 H). HRMS: calcd for $C_{22}H_{18}FN_3O_3 + H^+$, 392.140 50; found (ESI, $[M + H]^+$ obsd), 392.1407.

2-(3-(1-Benzyl-6-oxo-1,6-dihydropyridazin-3-yl)-2,5-dimethyl-1*H*-indol-1-yl)acetic Acid (16). Y = Me. Solid (overall yield, 15%). ^{1}H NMR (400 MHz, MeOD) δ 7.80 (d, J = 9.6 Hz, 1 H), 7.43−7.49 (m, 2 H), 7.28−7.41 (m, 4 H), 7.20 (d, J = 8.1 Hz, 1 H), 7.09 (d, J = 9.6 Hz, 1 H), 6.98−7.04 (m, 1 H), 5.43 (s, 2 H), 4.90 (s, 2 H), 2.44 (s, 3 H), 2.38 (s, 3 H). HRMS: calcd for $C_{23}H_{21}N_3O_3 + H^+$, 388.165 57; found (ESI, $[M + H]^+$ obsd), 388.1655.

2-(3-(1-Benzyl-6-oxo-1,6-dihydropyridazin-3-yl)-2-methyl-5-(methylsulfonyl)-1*H*-indol-1-yl)acetic Acid (17). 2-Methyl-5-(methylsulfonyl)-1*H*-indole was synthesized from 2-methyl-5-bromo-1*H*-indole according to the procedure described by Ma et al.[27] Y = Me. Solid (overall yield, 28%). ^{1}H NMR (400 MHz, MeOD) δ ppm 2.71 (s, 3 H), 3.31 (s, 3 H), 5.28 (s, 2 H), 5.64 (s, 2 H), 7.30 (d, J = 9.60 Hz, 1 H), 7.49−7.55 (m, 1 H), 7.56−7.63 (m, 2 H), 7.72−7.82 (m, 2 H), 7.93−8.01 (m, 2 H), 8.28−8.37 (m, 1 H), 8.60−8.63 (m, 1 H). HRMS calcd for ($C_{23}H_{21}N_3O_5S + H^+$), 452.1275; found, 452.1270.

2-(3-(1-Benzyl-6-oxo-1,6-dihydropyridazin-3-yl)-5-methoxy-2-methyl-1*H*-indol-1-yl)acetic Acid (18). Y = *t*-Bu. Solid (overall yield, 2.6%). ^{1}H NMR (DMSO-d_6) δ 7.75 (d, J = 9.6 Hz, 1H), 7.26−7.41 (m, 6H), 7.13 (d, J = 2.5 Hz, 1H), 7.05 (d, J = 9.6 Hz, 1H), 6.75 (dd, J = 8.8, 2.3 Hz, 1H), 5.35 (s, 2H), 4.89 (s, 2H), 3.65 (s, 3H), 2.38 (s, 3H). HRMS (ESI+) calcd for $C_{23}H_{22}N_3O_4$ (MH+) 404.1605; found, 404.1603. Anal. ($C_{23}H_{21}N_3O_4$) C, H, N.

2-(3-(1-Benzyl-6-oxo-1,6-dihydropyridazin-3-yl)-7-bromo-2-methyl-1*H*-indol-1-yl)acetic Acid (19). Y = Me. Solid (overall yield, 24%). ^{1}H NMR (400 MHz, $CDCl_3$) δ ppm 2.29 (s, 3 H), 5.33 (bs, 2 H), 5.35 (s, 2 H), 6.85−6.90 (m, 1 H), 7.11 (d, J = 9.60 Hz, 1 H), 7.21−7.29 (m, 4 H), 7.37−7.41 (m, 2 H), 7.43 (d, J = 9.60 Hz, 2 H). HRMS calcd for ($C_{22}H_{18}BrN_3O_3 + H^+$), 452.0604; found, 452.0590.

2-(3-(1-Benzyl-6-oxo-1,6-dihydropyridazin-3-yl)-5-chloro-7-fluoro-2-methyl-1*H*-indol-1-yl)acetic Acid (20). Y = Me. Solid (overall yield, 5%). ^{1}H NMR (DMSO-d_6) δ 13.37 (br s, 1H), 7.72 (d, J = 9.6 Hz, 1H), 7.42 (d, J = 1.3 Hz, 1H), 7.35−7.40 (m, 4H), 7.28−7.34 (m, 1H), 7.12 (dd, J = 12.4, 1.3 Hz, 1H), 7.07 (d, J = 9.6 Hz, 1H), 5.34 (s, 2H), 5.05 (s, 2H), 2.41 (s, 3H). HRMS (ESI+) calcd for $C_{22}H_{18}ClFN_3O_3$ (MH^+) 426.1015; found, 426.1016.

2-(3-(1-Benzyl-6-oxo-1,6-dihydropyridazin-3-yl)-5,7-dichloro-2-methyl-1*H*-indol-1-yl)acetic Acid (21). General procedure A was followed starting with 5,7-dichloro-2-methyl-1*H*-indole, which was prepared from 2,4-dichloroaniline according to Scheme 2.[18,19] Y = Me. Solid (overall yield, 35%). ^{1}H NMR (400 MHz, MeOD) δ ppm 2.62 (s, 3 H), 5.53 (s, 2 H), 5.63 (s, 2 H), 7.30 (d, J = 9.60 Hz, 1 H), 7.36 (d, J = 1.77 Hz, 1 H), 7.51−7.55 (m, 1 H), 7.56−7.62 (m, 2 H), 7.65−7.70 (m, 2 H), 7.71−7.74 (m, 1 H), 7.87 (d, J = 9.60 Hz, 1 H).

2-(3-(1-Benzyl-6-oxo-1,6-dihydropyridazin-3-yl)-5,7-difluoro-2-methyl-1*H*-indol-1-yl)acetic Acid (22). General procedure A was followed starting with 5,7-dichloro-2-methyl-1*H*-indole, which was prepared from 2,4-dichloroaniline according to Scheme 2.[18,19] Y = Me. Solid (overall yield, 24%). ^{1}H NMR (400 MHz, MeOD) δ ppm 2.61 (s, 3 H), 5.28 (s, 2 H), 5.63 (s, 2 H), 6.93−7.01

Table 7. PK Properties of 32 and 31

compd	species	iv Cl [a] ($mL\ min^{-1}\ kg^{-1}$)	$t_{1/2}$ [a] (h)	V_{ss} [a] (L/kg)	AUC_{0-inf} [b] ($h \cdot kg \cdot ng \cdot mL^{-1} \cdot mg^{-1}$)	C_{max} [b] (ng/mL)	bioavailability (%)
31	rat	13	4.3	1.7	3568	484	28
32	rat	12	3	1.6	5066	772	37
33	mouse	9	4	1.12	7526	1889	41

[a]Intravenous dose, 2 mg/kg. [b]Oral dose, 10 mg/kg.

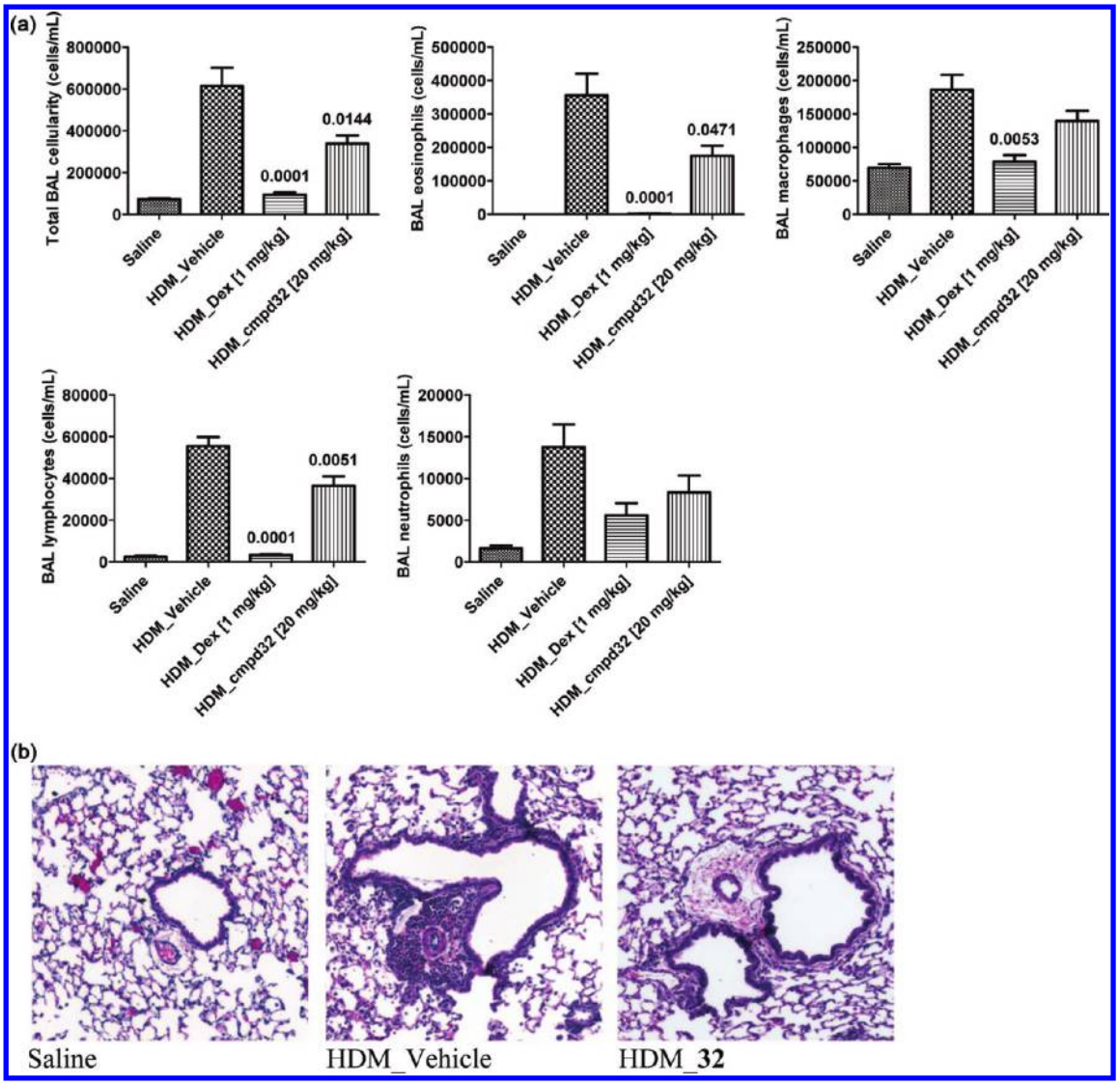

Figure 6. (a) Modulation of HDM-induced allergic airway disease in BALB/c mice. Total cellularity and eosinophil, macrophage, lymphocyte, neutrophil cell numbers in BAL samples were collected 72 h after HDM challenge. (b) H&E (hematoxylin and eosin) staining of mouse lung sections (magnification ×10). *P* values are given for comparisons between HDM-challenged mice treated with vehicle and HDM-challenged mice treated with compound **32**. Shown are the mean ± SEM from 8 to 20 mice per group.

(m, 1 H), 7.26−7.35 (m, 2 H), 7.49−7.60 (m, 3 H), 7.63−7.68 (m, 2 H), 7.91 (d, *J* = 9.60 Hz 1 H). HRMS calcd for ($C_{22}H_{17}F_2N_3O_3$ + H^+), 410.1311; found, 410.1311.

2-(3-(1-Benzyl-6-oxo-1,6-dihydropyridazin-3-yl)-7-chloro-5-fluoro-2-methyl-1*H*-indol-1-yl)acetic Acid (23). General procedure A was followed starting with 7-chloro-5-fluoro-2-methyl-1*H*-indole, which was prepared from 2-chloro-4-fluoroaniline according to Scheme 2 using literature procedure. Y = Me. Solid (overall yield, 31%). ^{1}H NMR (400 MHz, MeOD) δ ppm 2.62 (s, 3 H), 5.54 (s, 2 H), 5.63 (s, 2 H), 7.19 (dd, *J* = 9.09, 2.53 Hz, 1 H), 7.30 (d, *J* = 9.60 Hz, 1 H), 7.44 (dd, *J* = 9.35, 2.53 Hz, 1 H), 7.49−7.60 (m, 3 H), 7.63−7.68 (m, 2 H), 7.89 (d, *J* = 9.60 Hz, 1 H). HRMS calcd for ($C_{22}H_{17}ClFN_3O_3$ + H^+), 426.1015; found, 426.1014.

2-(3-(1-Benzyl-6-oxo-1,6-dihydropyridazin-3-yl)-5-fluoro-2-methyl-7-(methylsulfonyl)-1*H*-indol-1-yl)acetic Acid (24). General procedure A was followed starting with 7-(methylsulfonyl)-5-fluoro-2-methyl-1*H*-indole, which was prepared from 4-fluoro-2-(methylsulfonyl)aniline according to Scheme 2.[14,15] Y = Me. Solid (overall yield, 24%). ^{1}H NMR (400 MHz, DMSO-d_6) δ ppm 2.40 (s, 3 H), 3.49 (s, 3 H), 5.37 (s, 2 H), 5.43 (bs, 2 H), 7.10 (d, *J* = 9.60 Hz, 1 H), 7.30−7.36 (m, 1 H), 7.37 (s, 2 H), 7.38 (s, 2 H), 7.61 (dd, *J* = 9.60, 2.53 Hz, 1 H), 7.66 (dd, *J* = 8.84, 2.78 Hz, 1 H), 7.71 (d, *J* = 9.60 Hz, 1 H).

2-(3-(1-Benzyl-6-oxo-1,6-dihydropyridazin-3-yl)-7-fluoro-2-methyl-5-(methylsulfonyl)-1*H*-indol-1-yl)acetic Acid (25). General procedure A was followed starting with 7-fluoro-2-methyl-5-(methylsulfonyl)-1*H*-indole (**I-6-1**, general procedure B). Y = *t*-Bu. Solid (overall yield, 3.1%). ^{1}H NMR (DMSO-d_6) δ 13.65 (br s, 1H), 8.10 (d, *J* = 1.3 Hz, 1H), 7.78 (d, *J* = 9.9 Hz, 1H), 7.52 (dd, *J* = 11.9, 1.5 Hz, 1H), 7.42−7.47 (m, 2H), 7.34−7.41 (m, 2H), 7.27−7.33 (m, 1H), 7.12 (d, *J* = 9.6 Hz, 1H), 5.33 (s, 2H), 5.12 (s, 2H), 3.23 (s, 3H), 2.45 (s, 3H). HRMS (ESI+) calcd for $C_{23}H_{21}FN_3O_5S$ (MH^+) 470.1180; found, 470.1180. Anal. ($C_{23}H_{20}FN_3O_5S$) C, H, N.

2-(3-(1-Benzyl-6-oxo-1,6-dihydropyridazin-3-yl)-5-chloro-2-methyl-1*H*-indol-1-yl)acetic Acid (26). Solid (overall yield, 52%). Y = *t*-Bu. ^{1}H NMR (400 MHz, DMSO-d_6) δ 13.21 (br s, 1H), 8.38−8.43 (m, 1H), 7.85−7.94 (m, 2H), 7.56 (d, *J* = 8.6 Hz, 1H), 7.50−7.54 (m, 1H), 7.27−7.41 (m, 5H), 7.15 (dd, *J* = 8.7, 2.1 Hz, 1H), 7.11 (d, *J* = 2.0 Hz, 1H), 5.32−5.50 (m, 2H), 5.12 (s, 2H), 2.23 (s, 3H).

2-(3-(3-Benzyl-4-oxo-3,4-dihydrophthalazin-1-yl)-5-fluoro-2-methyl-1*H*-indol-1-yl)acetic Acid (28). Y = *t*-Bu. Solid (overall yield, 34%). ^{1}H NMR (400 MHz, DMSO-d_6) δ 13.20 (br s, 1H), 8.39−8.43 (m, 1H), 7.84−7.94 (m, 2H), 7.51−7.57 (m, 2H), 7.27−

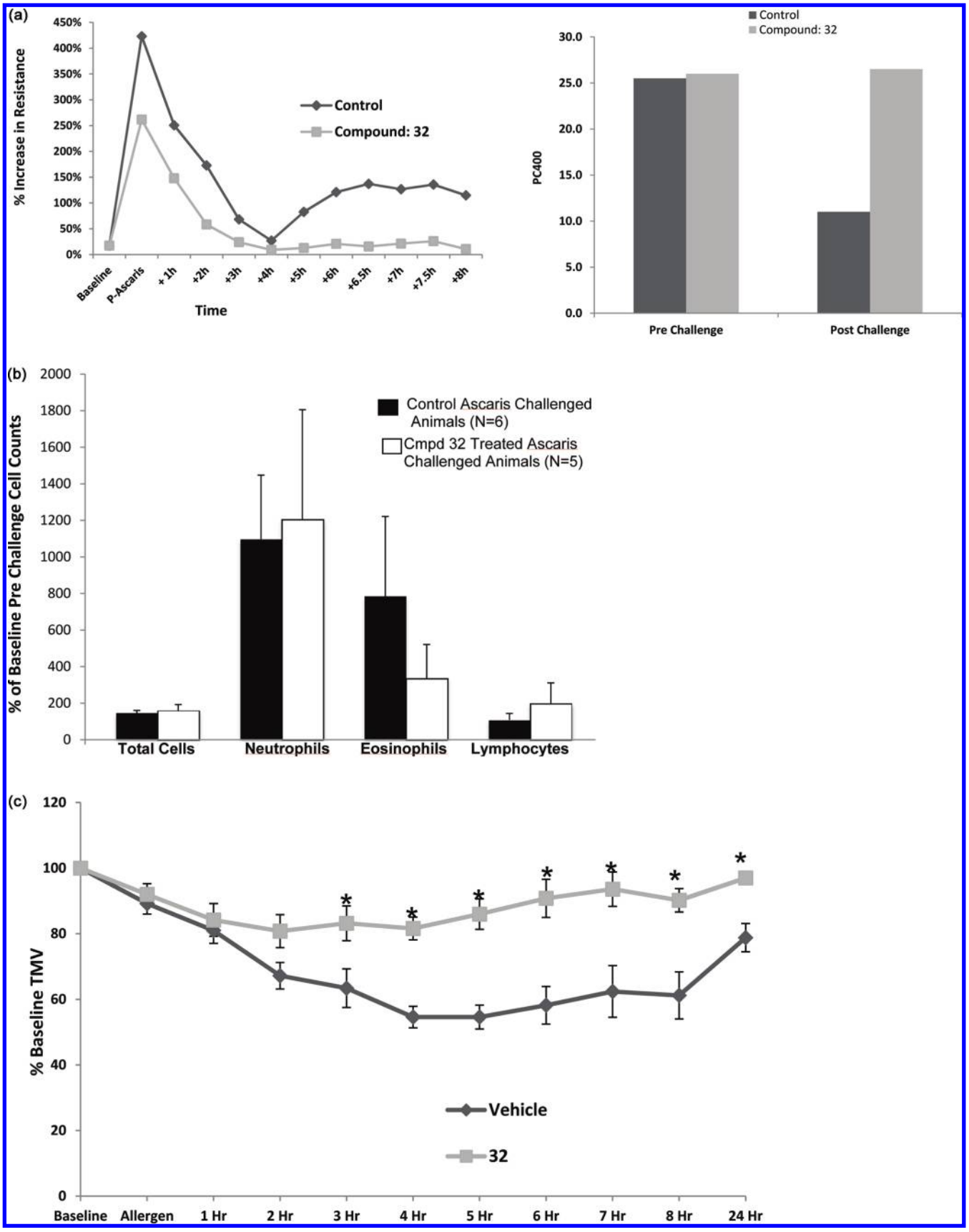

Figure 7. (a) Administration of compound **32** at 3 mg/kg iv in a sheep model of allergic airway bronchoconstriction and AHR: (i, top left) compound **32** attenuates EAR and blocks LAR; (ii, top right) compound **32** blocks AHR to aerosolized carbachol. (b) Compound **32** attenuates *Ascaris* induced BAL fluid eosinophilia at 1 mg/kg iv q.d. for 7 days in sheep. (c) Reduction in mucocilliary clearance in sheep with **32** at 3 mg/kg iv.

Table 8. Overall Profile of Compound 32

IC$_{50}$ (nM)						IC$_{50}$ (μM)	
hCRTH$_2$ FRET	hCRTH$_2$ binding	basophil chelmotaxis	hEOS	mCRTH$_2$ binding	DP$_1$ FRET	TXA$_2$ binding	Caco2 permeability at pH 6 (cm/s)
3	0.8	1.2	3	7	19000	560	7.1×10^{-6}

7.41 (m, 5H), 6.99 (td, J = 2.53, 9.22 Hz, 1H), 6.87 (dd, J = 2.53, 9.60 Hz, 1H), 5.43 (s, 2H), 5.11 (s, 2H), 2.23 (s, 3H). HRMS (ESI+) calcd for $C_{26}H_{21}N_3O_3$ (MH+) 442.1562; found, 442.1561.

2-(3-(1-(2,4-Difluorobenzyl)-6-oxo-1,6-dihydropyridazin-3-yl)-5-fluoro-2-methyl-1*H*-indol-1-yl)acetic Acid (34). Y = Me. Solid (overall yield, 23%). ^{1}H NMR (400 MHz, DMSO-d_6) δ 2.38 (s, 3 H), 5.05 (s, 3 H), 5.37 (s, 3 H), 6.97 (dt, J = 9.1, 2.5 Hz, 1 H), 7.06 (d, J = 9.6 Hz, 1 H), 7.11 (dt, J = 8.6, 2.5 Hz, 1 H), 7.18 (dd, J = 10.1, 2.5 Hz, 1 H), 7.28 (dt, J = 8.6, 2.5 Hz, 1 H), 7.42−7.55 (m, 2 H), 7.76 (d, J = 9.6 Hz, 1 H). HRMS: calcd for $C_{22}H_{16}F_3N_3O_3 + H^+$, 427.114 38 found (ESI-FTMS, $[M + H]^{1+}$), 427.113 98.

2-(3-(3-Benzyl-4-oxo-3,4,4a,5,6,7,8,8a-octahydrophthalazin-1-yl)-5-fluoro-2-methyl-1*H*-indol-1-yl)acetic Acid (29).[28] Y = Me. ^{1}H NMR (400 MHz, DMSO-d_6) δ 13.20 (br s, 1H), 7.70−7.66 (m, 2H), 7.39−7.35 (m, 4H), 7.27−7.15 (m, 2H), 5.11 (s, 2H), 4.15 (s, 2H), 2.64−2.4 (m, 2H), 2.23 (s, 3H), 1.8−1.6 (m, 1H), 1.55−1.36 (m, 7H).

General Procedure B (Scheme 2). Iodoaniline (I-5).[15] In a 250 mL round-bottomed flask substituted aniline (19.7 mmol) was taken up in dichloromethane. Bis(pyridine)iodonium(I) tetrafluoroborate (29.6 mmol) was added. Then trifluoromethanesulfonic acid (59 mmol) was added slowly via a syringe. LC−MS analysis 5 min after completion of this addition showed complete conversion to product. The reaction mixture was quenched with water and then partitioned between water and dichloromethane, and the aqueous layer was extracted with additional dichloromethane. The combined organic extracts were washed with 5% sodium thiosulfate, dried over anhydrous magnesium sulfate, filtered, evaporated, and purified by flash chromatography to give iodoaniline (**I-6**).[16]

In a 350 mL glass pressure vessel with a threaded Teflon cap, iodoaniline (12.0 mmol), copper iodide (0.16 mmol), and Pd-$(PPh_3)_2Cl_2$ (0.144 mmol) were taken up in 165 mL of triethylamine and cooled to −78 °C. Propyne (48 mmol) was condensed into a graduated cylinder and added to the reaction vessel. The vessel was then capped, the cooling bath removed, and the reaction mixture allowed to stir while warming to room temperature overnight behind a safety shield. Removal of the triethylamine by evaporation gave a crude material that was purified by flash chromatography over silica gel to give pure product.

5,7-Disubstituted-2-methyl-1*H*-indole (I-1).[16] Propynylaniline (10.9 mmol) was taken up in 210 mL of anhydrous DMF, and copper iodide (1.20 mmol) was added. The mixture was refluxed under nitrogen for 1 h until TLC analysis showed complete conversion to product. The reaction mixture was then evaporated, and the crude material was purified by flash chromatography over silica gel to give pure product.

2-Fluoro-6-iodo-4-(methylsulfonyl)aniline (I-5-1) . Yield, 49%. ^{1}H NMR (DMSO-d_6) δ 7.85 (dd, J = 1.8, 1.0 Hz, 1H), 7.56 (dd, J = 10.6, 2.0 Hz, 1H), 6.20 (s, 2H), 3.16 (s, 3H).

2-Fluoro-4-(methylsulfonyl)-6-(prop-1-yn-1-yl)aniline (I-6-1). Yield, 92%. ^{1}H NMR (DMSO-d_6) δ: 7.47 (dd, J = 10.9, 2.0 Hz, 1H), 7.43 (d, J = 2.0 Hz, 1H), 6.31 (s, 2H), 3.13 (s, 3H), 2.11 (s, 3H).

7-Fluoro-2-methyl-5-(methylsulfonyl)-1*H*-indole (I-1-1). Yield, 58%. ^{1}H NMR (DMSO-d_6) δ 12.01 (br s, 1H), 7.88 (d, J = 1.3 Hz, 1H), 7.36 (dd, J = 10.9, 1.5 Hz, 1H), 6.45−6.47 (m, 1H), 3.19 (s, 3H), 2.43 (d, J = 1.0 Hz, 3H).

4-Chloro-2-fluoro-6-iodoaniline (I-5-2). Yield, 91%. ^{1}H NMR ($CDCl_3$) δ 7.00−7.04 (m, 1H), 6.95 (dd, J = 10.6, 2.3 Hz, 1H), 4.18 (br s, 2H), 2.13 (s, 3H).

4-Chloro-2-fluoro-6-(prop-1-ynyl)aniline (I-6-2). Yield, 88%. ^{1}H NMR (DMSO-d_6) δ 11.58 (br s, 1H), 7.29 (d, J = 1.8 Hz, 1H), 6.94 (dd, J = 10.9, 1.8 Hz, 1H), 6.21 (ddd, J = 3.4, 1.9, 0.8 Hz, 1H), 2.38 (d, J = 0.8 Hz, 3H).

5-Chloro-7-fluoro-2-methyl-1*H*-indole (I-1-2). Yield, 52%. ^{1}H NMR (DMSO-d_6) δ: 12.33 (s, 1H), 7.98−8.02 (m, 1H), 7.89 (d, J = 9.1 Hz, 1H), 7.86 (d, J = 1.5 Hz, 1H), 7.16 (dd, J = 10.9, 1.8 Hz, 1H), 2.65 (s, 3H).

General Procedure C (Scheme 3). Amides of Compound 3. In a 25 mL round-bottomed flask, compound **3** (0.708 mmol), amine (2.83 mmol), and BOP (0.344 g, 0.779 mmol) were taken up in 6 mL of DMF. Base (3.60 mmol) was added, and the mixture was allowed to stir at room temperature over the weekend. It was then poured into 60 mL of water, and the off-white precipitate was collected, washed three times with water, dried under vacuum, and purified by flash chromatography over silica gel to give a solid.

2-(3-(3-Benzyl-4-oxo-3,4-dihydrophthalazin-1-yl)-2-methyl-1*H*-indol-1-yl)acetamide (4). General procedure C, ammonium chloride as the amine source, and 4-methylmorpholine as the base were used. Yield, 51%. ^{1}H NMR (DMSO-d_6) δ 8.37−8.42 (m, 1H), 7.82−7.92 (m, 2H), 7.70 (br s, 1H), 7.60 (dt, J = 7.8, 0.8 Hz, 1H), 7.43−7.47 (m, 1H), 7.26−7.41 (m, 6H), 7.10−7.18 (m, 2H), 6.99 (ddd, J = 8.0, 6.9, 1.0 Hz, 1H), 5.34−5.49 (m, 2H), 4.87 (s, 2H), 2.24 (s, 3H). HRMS (ESI+) calcd for $C_{26}H_{23}N_4O_2$ (MH^+) 423.1815; found, 423.1812.

2-(3-(3-Benzyl-4-oxo-3,4-dihydrophthalazin-1-yl)-2-methyl-1*H*-indol-1-yl)-*N*,*N*-dimethylacetamide (5). General procedure C, dimethylamine hydrochloride as the amine source, and 4-methylmorpholine as the base were used. Yield, 77%. ^{1}H NMR (DMSO-d_6) δ 8.37−8.43 (m, 1H), 7.83−7.92 (m, 2H), 7.57 (dt, J = 7.5, 0.9 Hz, 1H), 7.44−7.49 (m, 1H), 7.32−7.41 (m, 4H), 7.25−7.31 (m, 1H), 7.08−7.16 (m, 2H), 6.97 (td, J = 7.5, 0.8 Hz, 1H), 5.34−5.50 (m, 2H), 5.15−5.29 (m, 2H), 3.19 (s, 3H), 2.89 (s, 3H), 2.17 (s, 3H). HRMS (ESI+) calcd for $C_{28}H_{27}N_4O_2$ (MH^+) 451.2128; found, 451.2133.

2-Benzyl-4-(2-methyl-1-(2-oxo-2-(pyrrolidin-1-yl)ethyl)-1*H*-indol-3-yl)phthalazin-1(2*H*)-one (6). General procedure C, pyrrolidine as the amine source, and 4-methylmorpholine as the base were used. Yield, 79%. ^{1}H NMR (DMSO-d_6) δ 8.38−8.42 (m, 1H), 7.82−7.92 (m, J = 7.3, 7.3, 7.3, 7.3, 1.5 Hz, 2H), 7.55−7.60 (m, 1H), 7.46−7.51 (m, 1H), 7.32−7.42 (m, 4H), 7.25−7.31 (m, 1H), 7.09−7.15 (m, 2H), 6.94−7.01 (m, 1H), 5.35−5.50 (m, 2H), 5.07−5.20 (m, 2H), 3.68 (t, J = 6.8 Hz, 2H), 3.32−3.38 (m, 2H), 2.19 (s, 3H), 1.98 (quin, J = 6.8 Hz, 2H), 1.82 (quin, J = 6.8 Hz, 2H). HRMS (ESI+) calcd for $C_{30}H_{29}N_4O_2$ (MH^+) 477.2284; found, 477.2287.

2-(3-(3-Benzyl-4-oxo-3,4-dihydrophthalazin-1-yl)-2-methyl-1*H*-indol-1-yl)-*N*-(methylsulfonyl)acetamide (7). General procedure C, methanesulfonamide as the amine source, and diisopropylethylamine as the base were used. Yield, 7.4%. ^{1}H NMR (DMSO-d_6) δ 12.33 (br s, 1H), 8.35−8.46 (m, 1H), 7.82−7.95 (m, J = 7.3, 7.3, 7.3, 7.3, 1.5 Hz, 2H), 7.57 (dt, J = 7.6, 0.9 Hz, 1H), 7.46 (d, J = 8.1 Hz, 1H), 7.32−7.41 (m, 4H), 7.26−7.31 (m, 1H), 7.12−7.19 (m, 2H), 6.98−7.03 (m, 1H), 5.35−5.49 (m, 2H), 5.05 (s, 2H), 3.21 (s, 3H), 2.23 (s, 3H). HRMS (ESI+) calcd for $C_{27}H_{25}N_4O_4S$ (MH^+) 501.1590; found, 501.1581.

2-Benzyl-4-(1-(2-hydroxyethyl)-2-methyl-1*H*-indol-3-yl)-phthalazin-1(2*H*)-one (9). In a flame-dried two-necked 15 mL round-bottomed flask, under nitrogen, compound **3** (0.200 g, 0.472 mmol) and triethylamine (66 μL, 48 mg, 0.47 mmol) were taken up in 1.4 mL of anhydrous tetrahydrofuran and cooled to 0 °C with an ice−water bath. A solution of ethyl chloroformate (45 μL, 51 mg, 0.47 mmol) in 0.3 mL of anhydrous tetrahydrofuran was added dropwise via syringe. The mixture was stirred for 3 h, at which point sodium borohydride (36 mg, 0.95 mmol) was added, and the ice bath was removed. The mixture was stirred for 25 min. LC−MS analysis showed the presence of the desired product but no mixed anhydride

intermediate or acid starting material. The reaction mixture was partitioned between 5 mL each of ethyl acetate and brine, and the aqueous layer was extracted with additional ethyl acetate. The combined organic extracts were washed with 5 mL of brine, dried over anhydrous magnesium sulfate, filtered, evaporated, and purified by flash chromatography over silica gel (12−100% ethyl acetate in hexanes). Additional purification by preparative HPLC (water/acetonitrile with 0.1% formic acid), followed by lyophilization, gave pure product (29 mg, 15% yield). ^{1}H NMR (DMSO-d_6) δ 8.36−8.42 (m, 1H), 7.80−7.92 (m, J = 18.4, 7.4, 7.4, 1.4 Hz, 2H), 7.59 (dt, J = 7.8, 0.8 Hz, 1H), 7.52 (d, J = 8.1 Hz, 1H), 7.32−7.40 (m, 4H), 7.26−7.31 (m, 1H), 7.09−7.17 (m, 2H), 6.97 (ddd, J = 8.0, 7.1, 0.9 Hz, 1H), 5.34−5.49 (m, 2H), 4.97 (t, J = 5.3 Hz, 1H), 4.30 (t, J = 5.7 Hz, 2H), 3.75 (q, J = 5.2 Hz, 2H), 2.33 (s, 3H). HRMS (ESI+) calcd for $C_{26}H_{24}N_3O_2$ (MH^+) 410.1862; found, 410.1872.

4-(1-((2*H*-Tetrazol-5-yl)methyl)-2-methyl-1*H*-indol-3-yl)-2-benzylphthalazin-1(2*H*)-one (8) (Scheme 4). 1-Chloro-4-(2-methyl-1*H*-indol-3-yl)phthalazine (I-2-1). The procedure described above for **I-2** was followed, reacting 2-methylindole with 1,4-dichlorophthalazine. Yield, 74%. ^{1}H NMR (DMSO-d_6) δ 11.68 (s, 1H), 8.34−8.40 (m, 1H), 8.16 (ddd, J = 8.3, 7.1, 1.3 Hz, 1H), 8.03−8.08 (m, 1H), 7.96 (dq, J = 8.3, 0.7 Hz, 1H), 7.45 (dt, J = 8.1, 0.9 Hz, 1H), 7.10−7.19 (m, 2H), 6.99 (ddd, J = 7.9, 7.0, 1.0 Hz, 1H), 2.42 (s, 3H).

2-(3-(4-Chlorophthalazin-1-yl)-2-methyl-1*H*-indol-1-yl)-acetonitrile (I-7). The procedure described above for **I-3** was followed, reacting **I-2-1** with bromoacetonitrile. Yield, 35%. ^{1}H NMR (DMSO-d_6) δ 8.37−8.42 (m, 1H), 8.18 (ddd, J = 8.3, 7.1, 1.0 Hz, 1H), 8.06 (ddd, J = 8.3, 7.1, 1.3 Hz, 1H), 7.87−7.91 (m, 1H), 7.74−7.79 (m, 1H), 7.31 (ddd, J = 8.2, 7.1, 1.1 Hz, 1H), 7.20−7.24 (m, 1H), 7.09−7.14 (m, 1H), 5.71 (s, 2H), 2.46 (s, 3H).

2-(3-(4-Hydroxyphthalazin-1-yl)-2-methyl-1*H*-indol-1-yl)-acetonitrile (I-8). The procedure described above for **I-4** was followed. Yield, 67%. ^{1}H NMR (DMSO-d_6) δ 12.82 (s, 1H), 8.35 (dd, J = 7.7, 1.4 Hz, 1H), 7.80−7.90 (m, J = 7.4, 7.4, 7.4, 7.4, 1.5 Hz, 2H), 7.70 (d, J = 8.1 Hz, 1H), 7.48 (dd, J = 6.7, 1.4 Hz, 1H), 7.27 (t, J = 8.0 Hz, 1H), 7.21 (d, J = 7.6 Hz, 1H), 7.05−7.13 (m, 1H), 5.64 (s, 2H), 2.41 (s, 3H).

2-(3-(3-Benzyl-4-oxo-3,4-dihydrophthalazin-1-yl)-2-methyl-1*H*-indol-1-yl)acetonitrile (I-9). **I-8** (0.250 g, 0.795 mmol) was taken up in 15 mL of DMF, and potassium carbonate (0.385 g, 2.78 mmol) and benzyl bromide (0.28 mL, 0.41 g, 2.4 mmol) were added. The mixture was heated at 100 °C for 1.5 h until LC−MS analysis showed complete consumption of starting material. The crude product was purified by flash chromatography over silica gel (7−60% ethyl acetate in hexanes) to give pure product (0.236 g, 73% yield). ^{1}H NMR (DMSO-d_6) δ 8.38−8.43 (m, 1H), 7.82−7.93 (m, J = 19.1, 7.4, 7.4, 1.5 Hz, 2H), 7.68−7.73 (m, 1H), 7.52−7.57 (m, 1H), 7.32−7.41 (m, 4H), 7.23−7.32 (m, 2H), 7.15−7.20 (m, 1H), 7.04−7.11 (m, 1H), 5.64 (s, 2H), 5.33−5.51 (m, 2H), 2.36 (s, 3H).

Compound 8. In a 10 mL round-bottomed flask, **I-9** (0.236 g, 0.583 mmol), zinc bromide (0.131 g, 0.583 mmol), and sodium azide (42 mg, 0.642 mmol) were taken up in 3 mL of isopropanol and 1.2 mL of water.[29] The mixture was refluxed overnight until LC−MS analysis showed complete conversion to product, and it was cooled to room temperature. It was partitioned between ethyl acetate and 2 M hydrochloric acid, and the aqueous layer was extracted with additional ethyl acetate. The combined organic extracts were evaporated, and the residue was taken up in 40 mL of 0.25 M NaOH and stirred for 2 h. Although the reference had suggested that a precipitate of zinc hydroxide would form, only a faint cloudiness that could not be removed by filtration was observed. Thus, the filtered (and still cloudy) solution was acidified with concentrated hydrochloric acid and the off-white precipitate collected, washed three times with 2 M hydrochloric acid, and dried under vacuum. It was then purified by preparative HPLC (water/acetonitrile with 0.1% formic acid) and lyophilized to give pure product (0.120 g, 46% yield). ^{1}H NMR (DMSO-d_6) δ 8.37−8.42 (m, 1H), 7.81−7.92 (m, J = 18.4, 7.4, 7.4, 1.4 Hz, 2H), 7.55−7.62 (m, 2H), 7.32−7.41 (m, 4H), 7.25−7.31 (m, 1H), 7.10−7.19 (m, 2H), 6.95−7.04 (m, 1H), 5.80 (s, 2H), 5.34−5.49 (m, 2H), 2.37 (s, 3H). HRMS (ESI+) calcd for $C_{26}H_{22}N_7O$ (MH^+) 448.1880; found, 448.1876.

General Procedure C (Scheme 5). Intermediate I-10. In a 500 mL two-necked round-bottomed flask, 5-substituted-2-methylindole (33.3 mmol) was taken up 100 mL of anhydrous DMF, under nitrogen. Sodium hydride (1.69 g of a 60 wt % suspension in mineral oil, 42.2 mmol) was added in small aliquots, and the mixture was allowed to stir at room temperature for 30 min. Methyl bromoacetate (42 mmol) was added all at once by syringe, and the mixture was allowed to stir overnight. It was then quenched by addition of 20 mL of brine, via syringe, and partitioned between 400 mL each of ethyl acetate and brine. The aqueous layer was extracted with additional ethyl acetate (2×), and the combined organic extracts were washed with brine (3×), dried over anhydrous magnesium sulfate, filtered, evaporated, and purified by flash chromatography over silica gel.

Intermediate I-11. To a 500 mL round-bottom flask under an atmosphere of nitrogen were added **I-10** (16.1 mmol), 6-oxo-1,6-dihydropyridazine-3-carbaldehyde or **I-14** or **I-15** (16.1 mmol), and 200 mL of anhydrous methylene chloride. The resulting solution was cooled to 0 °C in an ice−water bath, and triethylsilane (56.4 mmol) and trifluoroacetic acid (48.3 mmol) were added dropwise. The mixture was allowed to warm to room temperature and then stirred for 24 h. The mixture was then poured into saturated sodium bicarbonate$_{(aq)}$ and the aqueous layer extracted with two 50 mL portions of methylene chloride. The combined organic layers were then washed with water and brine and dried over magnesium sulfate. Filtration and removal of solvent in vacuo gave the crude material which was then purified by silica gel chromatography.

Intermediate I-12.[17] To a 100 mL round-bottom flask under a nitrogen atmosphere were added **I-11** (6.16 mmol), substituted benzyl bromide (12.33 mmol), potassium carbonate (18.49 mmol), and 50 mL of DMF. The resulting suspension was heated to 85 °C for 16 h. The mixture was then allowed to cool to room temperature and then poured into 200 mL of water. This was extracted with three 50 mL portions of ethyl acetate. The combined organic layers were washed with water and brine and dried over $MgSO_4$. Filtration and concentration in vacuo gave a tan solid. The crude material was purified by silica gel chromatography.

Intermediate I-13. To a mixture of **I-11** (1.47 mmol), substituted benzyl alcohol (2.21 mmol), triphenylphosphine (4.42 mmol), and 8 mL of dry DMF was added diisopropyl diazene-1,2-dicarboxylate (4.42 mmol) at 25 °C. The reaction mixture was stirred at 80 °C for 16 h. Water (30 mL) and ethyl acetate (50 mL) were added. The organic layer was washed with brine, dried over magnesium sulfate, and filtered and the solvent removed in vacuo to give an oil.

Pyridazine Linker (Scheme 5). To a 100 mL round-bottom flask were added **I-12** or **I-13** (5.16 mmol) and 20 mL of THF. To this was added a solution of lithium hydroxide (25.8 mmol) in 10 mL of water. To the resulting biphasic mixture was added methanol dropwise until a single layer formed. The resulting solution was stirred for 2 h at room temperature. It was then poured into 1.2 N HCl$_{(aq)}$, and the aqueous layer was extracted with three 50 mL portions of ethyl acetate. The combined organic layers were washed with water and brine and dried over magnesium sulfate. Filtration and removal of solvent in vacuo gave the crude material. This was purified by column or reverse phase HPLC.

General Procedure D (Scheme 6). Methyl 6-Oxo-1,4,5,6-tetrahydropyridazine-3-carboxylate (I-16). To a 100 mL round-bottom flask equipped with a condenser was added dimethyl 2-oxopentanedioate (5.00 g, 28.71, 1.0 equiv), methanol (30 mL, 0.1 M), hydrazine (0.99 mL, 31.03 mmol, 1.1 equiv), and 7 drops of acetic acid. The mixture was heated to reflux and stirred under nitrogen for 5 h. The mixture was allowed to cool to room temperature and then was concentrated in vacuo yielding **I-16**, methyl 6-oxo-1,4,5,6-tetrahydropyridazine-3-carboxylate, as a white solid in quantitative yield. ^{1}H NMR (400 MHz, DMSO-d_6) δ 11.26 (br s, 1 H), 3.75 (s, 3 H), 2.71−2.80 (m, 2 H), 2.38−2.47 (m, 2 H).

Intermediate I-17. To a 100 mL round-bottom flask which contained **I-16**, methyl 6-oxo-1,4,5,6-tetrahydropyridazine-3-carboxylate (8.01 mmol), were added potassium carbonate (20.02 mmol)

and DMF (80 mL, 0.1 M). The flask was purged with nitrogen. Substituted benzyl bromide (16.02 mmol) was added and the mixture stirred at 90 °C overnight. The mixture was cooled to room temperature, extracted with ethyl acetate, washed with brine, dried over $MgSO_4$, and concentrated in vacuo. The resulting material was purified via silica gel chromatography.

Intermediate I-18. To a 100 mL round-bottom flask equipped with a condenser were added **I-17** (3.05 mmol), THF (12 mL, 0.25 M), methanol (2.4 mL, 1.25 M), and sodium borohydride (3.05 mmol). The mixture was heated to reflux and stirred under nitrogen for 5 h. The mixture was cooled to room temperature, extracted with ethyl acetate, washed with brine, dried over $MgSO_4$, and concentrated in vacuo, resulting in **I-18.**

Intermediate I-14. To a 100 mL round-bottom flask equipped with a condenser were added **I-18** (0.918 mmol and toluene (20 mL, 0.05 M). Manganese dioxide (13.77 mmol) was added slowly, and the mixture was heated to reflux and stirred under nitrogen overnight. The mixture was cooled to room temperature and filtered through Celite, resulting in **I-14.**

Intermediate I-15. In a two-necked 100 mL round-bottomed flask fitted with an addition funnel, under nitrogen, oxalyl chloride (6.4 mmol) was taken up in 11 mL of anhydrous dichloromethane, and the solution was cooled to −78 °C (dry ice/acetone bath). A solution of dimethyl sulfoxide (13 mmol) in 3 mL of anhydrous dichloromethane was added in rapid drops from the addition funnel. The reaction mixture was stirred for 20 min. Then a solution of **I-18** (4.00 mmol) in 3 mL of anhydrous dichloromethane was added over 10 min. The reaction mixture was now stirred for 1 h at −78 °C. Triethylamine (28 mmol) was added dropwise, and stirring continued for an additional 20 min. Stirring became quite difficult because of the formation of a thick precipitate. The cooling bath was removed, and the mixture was allowed to warm to room temperature. Water (20 mL) was added, and the layers were separated. The aqueous layer was extracted with additional dichloromethane (2 × 10 mL), and the combined organic extracts were washed with brine (2 × 10 mL). The dichloromethane solution was dried over anhydrous magnesium sulfate, filtered, and evaporated. The residue was taken up in 75 mL of dichloromethane and washed successively with 20 mL each of 0.5 M hydrochloric acid, water, 5% sodium carbonate, water, and brine. The solution was then dried over anhydrous magnesium sulfate, filtered, and evaporated to give **I-15**.

6-Oxo-1-(2,4,5-trifluorobenzyl)-1,6-dihydropyridazine-3-carbaldehyde (I-14-1). General procedure D was used. Overall yield, 6%. ^{1}H NMR (400 MHz, $CDCl_3$) δ 9.66 (d, 1 H), 7.70 (dd, J = 9.7, 2.1 Hz, 1 H), 7.03−7.21 (m, 1 H), 6.81−6.99 (m, 2 H), 5.34 (s, 2 H).

6-Oxo-1-(4-(trifluoromethyl)benzyl)-1,6-dihydropyridazine-3-carbaldehyde (I-14-2). General procedure D was used. Overall yield, 15%. ^{1}H NMR (400 MHz, $CDCl_3$) δ 5.45 (s, 2 H), 7.00 (dd, J = 9.7, 0.9 Hz, 1 H), 7.53−7.68 (m, 4 H), 7.75 (d, J = 9.6 Hz, 1 H), 9.75 (d, J = 1.0 Hz, 1 H).

1-Benzyl-6-oxo-1,6-dihydropyridazine-3-carbaldehyde (I-14-3). General procedure D was used. Overall yield, 20%. ^{1}H NMR (400 MHz, $CDCl_3$) δ 5.41 (s, 2 H), 6.97 (dd, J = 9.7, 0.9 Hz, 1 H), 7.29−7.39 (m, 3 H), 7.46 (d, J = 1.5 Hz, 1 H), 7.48 (d, J = 2.0 Hz, 1 H), 7.72 (d, J = 9.6 Hz, 1 H), 9.75 (d, J = 1.0 Hz, 1 H).

1-Benzyl-6-oxo-1,4,5,6-tetrahydropyridazine-3-carbaldehyde (I-15-1). General procedure D was used. Overall yield, 36%. ^{1}H NMR (DMSO-d_6) δ 9.42 (s, 1H), 7.19−7.45 (m, 5H), 4.99 (s, 2H), 2.69−2.75 (m, 2H), 2.56−2.63 (m, 2H).

1-(2,4-Difluorobenzyl)-6-oxo-1,4,5,6-tetrahydropyridazine-3-carbaldehyde (I-15-2). General procedure D was used. Overall yield, 49%. A mixture of **I-14-4** (1-(2,4-difluorobenzyl)-6-oxo-1,6-dihydropyridazine-3-carbaldehyde) and **I-15-2** was obtained. No attempt was made to separate the two at this stage because of stability concerns. The compounds were purified in the final step. **I-14-4**: ^{1}H NMR (DMSO-d_6) δ 9.64 (d, J = 1.0 Hz, 1H), 7.80 (d, J = 9.6 Hz, 1H), 7.43 (td, J = 8.7, 6.6 Hz, 1H), 7.29 (ddd, J = 10.6, 9.3, 2.5 Hz, 1H), 7.05−7.12 (m, 2H), 5.39 (s, 2H). **I-15-2**: ^{1}H NMR (DMSO-d_6) δ 9.40 (s, 1H), 5.00 (s, 2H), 2.69−2.74 (m, 2H), 2.56−2.61 (m, 2H). Aromatic ^{1}H NMR peaks overlap with those for **I-14-4**.

{3-[(1-Benzyl-6-oxo-1,6-dihydropyridazin-3-yl)methyl]-5-fluoro-2-methyl-1*H*-indol-1-yl}acetic Acid (30). Scheme 5a was used. Solid (overall yield, 5%). ^{1}H NMR (400 MHz, DMSO-d_6) δ 13.02 (br s, 1H), 7.27−7.39 (m, 6H), 7.14−7.21 (m, 2H), 6.82−6.91 (m, 2H), 5.22 (s, 2H), 4.94 (s, 2H), 3.96 (s, 2H), 2.30 (s, 3H)

2-(3-((1-Benzyl-6-oxo-1,4,5,6-tetrahydropyridazin-3-yl)-methyl)-5-fluoro-2-methyl-1*H*-indol-1-yl)acetic Acid (31). General procedure C and Scheme 5d were followed using **I-15-1** (prepared using general procedure D). Overall yield, 50%. ^{1}H NMR (DMSO-d_6) δ 12.99 (s, 1H), 7.36 (dd, J = 8.8, 4.5 Hz, 1H), 7.28−7.34 (m, 2H), 7.22−7.28 (m, 3H), 7.14 (dd, J = 9.9, 2.5 Hz, 1H), 6.87 (td, J = 9.2, 2.5 Hz, 1H), 4.94 (s, 2H), 4.84 (s, 2H), 3.65 (s, 2H), 2.26−2.32 (m, 4H), 2.24 (s, 3H). HRMS (ESI+) calcd for $C_{23}H_{23}FN_3O_3$ (MH^+) 408.1718; found, 408.1714. Anal. ($C_{23}H_{22}FN_3O_3 \cdot {}^1/_2H_2O$) C, H, N.

2-(3-((1-(2,4-Difluorobenzyl)-6-oxo-1,6-dihydropyridazin-3-yl)methyl)-5-fluoro-2-methyl-1*H*-indol-1-yl)acetic Acid (32). Scheme 5a was used. Solid (overall yield, 18%). ^{1}H NMR (400 MHz, DMSO-d_6) δ 2.28 (s, 3 H), 3.91 (s, 2 H), 4.94 (s, 2 H), 5.25 (s, 2 H), 6.80−6.91 (m, 2 H), 7.03 (m, J = 8.6, 8.6, 2.6, 1.0 Hz, 1 H), 7.09 (dd, J = 9.7, 2.4 Hz, 1 H), 7.17 (d, J = 9.6 Hz, 1 H), 7.21−7.28 (m, 1 H), 7.28−7.38 (m, 2 H), 13.00 (s, 1 H). HRMS: calcd for $C_{23}H_{18}F_3N_3O_3$ + H^+, 441.130 03 found (ESI-FTMS, $[M + H]^{1+}$), 441.130 13.

2-(3-((1-(2,4-Difluorobenzyl)-6-oxo-1,4,5,6-tetrahydropyridazin-3-yl)methyl)-5-fluoro-2-methyl-1*H*-indol-1-yl)acetic Acid (33). General procedure C and Scheme 5d were followed using **I-15-2** (prepared using general procedure D). Overall yield, 62%. ^{1}H NMR (DMSO-d_6) δ 7.25−7.35 (m, 2H), 7.17−7.24 (m, 1H), 6.97−7.05 (m, 2H), 6.85 (td, J = 9.2, 2.4 Hz, 1H), 4.86 (s, 4H), 3.63 (s, 2H), 2.29 (s, 4H), 2.23 (s, 3H). HRMS (ESI+) calcd for $C_{23}H_{21}F_3N_3O_3$ (MH^+) 444.1530; found, 444.1530.

2-(5-Fluoro-3-((1-(4-(2-hydroxypropan-2-yl)benzyl)-6-oxo-1,6-dihydropyridazin-3-yl)methyl)-2-methyl-1*H*-indol-1-yl)-acetic Acid (35). General procedure C and Scheme 5a were followed using 2-(4-(bromomethyl)phenyl)propan-2-ol.[30] Solid (overall yield, 30%). ^{1}H NMR (400 MHz, MeOD) δ ppm 1.40 (s, 6 H), 2.24 (s, 3 H), 3.92 (s, 2 H), 4.79 (s, 2 H), 5.20 (s, 2 H), 6.71 (d, J = 9.35 Hz, 1 H), 6.71−6.77 (m, 1 H), 6.99 (dd, J = 9.60, 2.27 Hz, 1 H), 7.10 (d, J = 9.35 Hz, 1 H), 7.09−7.13 (m, 1 H), 7.22 (d, J = 8.59 Hz, 2 H), 7.32−7.36 (m, 2 H). HRMS (ESI+) calcd for $C_{26}H_{26}FN_3O_4$ (MH^+) 464.1980; found, 464.1981

2-(5-Fluoro-3-((1-((4-fluoropyridin-3-yl)methyl)-6-oxo-1,6-dihydropyridazin-3-yl)methyl)-2-methyl-1*H*-indol-1-yl)acetic Acid (36). General procedure C and Scheme 5b were followed using 2-(3-fluoropyridin-4-yl)methanol (prepared from 3-fluoroisonicotinaldehyde).[31] Solid (overall yield, 18%). ^{1}H NMR (400 MHz, MeOD) δ ppm 2.38 (s, 3 H), 4.04 (s, 2 H), 4.84 (s, 2 H), 5.50 (s, 2 H), 6.82−6.91 (m, 2 H), 7.00−7.05 (m, 1 H), 7.20−7.26 (m, 2 H), 7.29−7.34 (m, 1 H), 8.30−8.34 (m, 1 H), 8.46−8.50 (m, 1 H). HRMS: calcd for ($C_{22}H_{18}F_2N_4O_3$ + H^+), 425.1420; found, 425.1419.

2-(5-Fluoro-2-methyl-3-((6-oxo-1-(2,4,5-trifluorobenzyl)-1,6-dihydropyridazin-3-yl)methyl)-1*H*-indol-1-yl)acetic Acid (37). General procedure C and Scheme 5c were followed using **I-14-1** (prepared using general procedure D). Solid (overall yield, 20%). ^{1}H NMR (400 MHz, DMSO-d_6) δ 7.52−7.60 (m, 1 H), 7.30−7.38 (m, 2 H), 7.18 (d, J = 9.6 Hz, 1 H), 7.03 (dd, J = 10.0, 2.4 Hz, 1 H), 6.82−6.89 (m, 2 H), 5.24 (s, 2 H), 4.89 (s, 2 H), 3.91 (s, 2 H), 2.29 (s, 3 H). HRMS: calcd for $C_{23}H_{17}F_4N_3O_3$ + H^+, 460.127 88; found (ESI, $[M + H]^+$ obsd), 460.1276.

2-(3-((1-Benzyl-6-oxo-1,6-dihydropyridazin-3-yl)methyl)-5-chloro-2-methyl-1*H*-indol-1-yl)acetic Acid (38). Scheme 5c was used. Solid (overall yield, 17%). ^{1}H NMR (400 MHz, DMSO-d_6) δ 2.31 (s, 3 H), 3.98 (s, 2 H), 4.95 (s, 2 H), 5.21 (s, 2 H), 6.85 (d, J = 9.6 Hz, 1 H), 7.05 (dd, J = 8.7, 2.1 Hz, 1 H), 7.16 (d, J = 9.6 Hz, 1 H), 7.24−7.36 (m, 5 H), 7.39 (d, J = 8.8 Hz, 1 H), 7.49 (d, J = 2.3 Hz, 1 H). HRMS: calcd for $C_{23}H_{20}ClN_3O_3$ + H^+, 421.119 32; found (ESI-FTMS, $[M + H]^{1+}$), 421.119 12.

(3-{[1-(2,4-Difluorobenzyl)-6-oxo-1,6-dihydropyridazin-3-yl]methyl}-2-methyl-1*H*-indol-1-yl)acetic Acid (39). Scheme 5a was used. Solid (overall yield, 43%). ^{1}H NMR (400 MHz, DMSO-d_6) δ 12.99 (br s, 1H), 7.21−7.46 (m, 4H), 7.14 (d, J = 9.60 Hz, 1H),

6.96−7.10 (m, 2H), 6.78−6.94 (m, 2H), 5.26 (s, 2H), 4.92 (s, 2H), 3.93 (s, 2H), 2.30 (s, 3H). HRMS: calcd for ($C_{23}H_{19}F_2N_3O_3$ + H^+), 424.1466; found, 424.1455.

2-(5-Fluoro-2-methyl-3-((6-oxo-1-(pyridin-3-ylmethyl)-1,6-dihydropyridazin-3-yl)methyl)-1*H*-indol-1-yl)acetic Acid (40). Scheme 5a was used. Solid (overall yield, 11.7%). ^{1}H NMR (400 MHz, DMSO-d_6) δ 8.57 (d, J = 2.3 Hz, 1 H), 8.50 (dd, J = 4.9, 1.6 Hz, 1 H), 7.69 (dt, J = 7.8, 2.1 Hz, 1 H), 7.31−7.41 (m, 2 H), 7.12−7.20 (m, 2 H), 6.81−6.91 (m, 2 H), 5.26 (s, 2 H), 4.89 (s, 2 H), 3.95 (s, 2 H), 2.29 (s, 3 H). HRMS: calcd for $C_{22}H_{19}FN_4O_3$ + H^+, 407.151 40; found (ESI, $[M + H]^+$ obsd), 407.1514.

2-(5-Fluoro-2-methyl-3-((6-oxo-1-(4-(trifluoromethyl)-benzyl)-1,6-dihydropyridazin-3-yl)methyl)-1*H*-indol-1-yl)acetic Acid (41). General procedure C and Scheme 5c were followed using **I-14-2** (prepared using general procedure D). Solid (overall yield, 30%). ^{1}H NMR (400 MHz, DMSO-d_6) δ 2.31 (s, 3 H), 3.95 (s, 2 H), 4.94 (s, 2 H), 5.32 (s, 2 H), 6.82−6.91 (m, 2 H), 7.11 (dd, J = 9.9, 2.5 Hz, 1 H), 7.19 (d, J = 9.6 Hz, 1 H), 7.35 (dd, J = 8.8, 4.3 Hz, 1 H), 7.49 (d, J = 8.1 Hz, 2 H), 7.69 (d, J = 8.1 Hz, 2 H). HRMS: calcd for $C_{24}H_{19}F_4N_3O_3$ + H^+, 473.136 25 found (ESI-FTMS, $[M + H]^{1+}$), 473.136 25.

2-(5-Fluoro-3-((1-(4-(1,1,1,3,3,3-hexafluoro-2-hydroxypropan-2-yl)benzyl)-6-oxo-1,6-dihydropyridazin-3-yl)methyl)-2-methyl-1*H*-indol-1-yl)acetic Acid (42). Scheme 5a was used. Solid (overall yield, 35%). ^{1}H NMR (400 MHz, MeOD) δ ppm 2.35 (s, 3 H), 4.06 (s, 2 H), 4.84 (s, 2 H), 5.39 (s, 2 H), 6.83−6.89 (m, 1 H), 6.86 (d, J = 9.60 Hz, 1 H), 7.14 (dd, J = 9.85, 2.53 Hz, 1 H), 7.23 (dd, J = 8.84, 4.29 Hz, 1 H), 7.27 (d, J = 9.60 Hz, 1 H), 7.48 (d, J = 8.59 Hz, 2 H), 7.71 (d, J = 8.34 Hz, 2 H).

2-(3-((1-Benzyl-6-oxo-1,6-dihydropyridazin-3-yl)methyl)-2-methyl-1*H*-indol-1-yl)acetic Acid (43). General procedure C and Scheme 5c were followed using **I-14-3** (prepared using general procedure D). Solid (overall yield, 50%). ^{1}H NMR (400 MHz, DMSO-d_6) δ 2.32 (s, 3 H), 3.97 (s, 2 H), 4.93 (s, 2 H), 5.24 (s, 2 H), 6.83 (d, J = 9.6 Hz, 1 H), 6.87−6.95 (m, 1 H), 6.99−7.07 (m, 1 H), 7.12 (d, J = 9.3 Hz, 1 H), 7.24−7.42 (m, 7 H). HRMS: calcd for $C_{23}H_{21}N_3O_3$ + H^+, 387.158 29; found (ESI-FTMS, $[M + H]^{1+}$ 387.158 09.

2-(3-((1-(2,4-Difluorobenzyl)-6-oxo-1,6-dihydropyridazin-3-yl)methyl)-5,7-difluoro-2-methyl-1*H*-indol-1-yl)acetic Acid (44). Scheme 5a was followed starting with 5,7-difluoro-2-methyl-1*H*-indole, which was prepared from 2,4-difluoroaniline according to Scheme 2.[14,15] Solid (overall yield, 48%). ^{1}H NMR (400 MHz, MeOD) δ ppm 2.22 (s, 3 H), 3.86 (s, 2 H), 4.84 (s, 2 H), 5.24 (s, 2 H), 6.49−6.56 (m, 1 H), 6.70−6.86 (m, 3 H), 6.74 (d, J = 9.60 Hz, 1 H), 7.11 (d, J = 9.60 Hz, 1 H), 7.18−7.26 (m, 1H).

2-(3-((3-Benzyl-4-oxo-3,4-dihydrophthalazin-1-yl)methyl)-5-chloro-2-methyl-1*H*-indol-1-yl)acetic Acid (27) (Scheme 7). Methyl 2-(5-Chloro-2-methyl-1*H*-indol-3-yl)acetate (I-19). To a 250 mL round-bottom flask under an atmosphere of nitrogen was added 5-chloro-2-methylindole (5.0 g, 30.2 mmol, 1.0 equiv) and 100 mL of THF. The resulting solution was cooled to −78 °C in a dry ice/acetone bath, and *n*-butyllithium (21 mL of 1.51 M solution, 31.72 mmol, 1.05 equiv) was added dropwise over 30 min. This was allowed to stir at −78 °C for 30 min, at which point zinc chloride (4.12 g, 30.2 mmol, 1.0 equiv) was added as a solution in 5 mL of THF dropwise. The resulting mixture was allowed to warm to room temperature. Methyl bromoacetate (2.78 mL, 30.2 mmol, 1.0 equiv) was then added and the mixture allowed to stir for 24 h. The reaction mixture was then poured into 500 mL of saturated aqueous ammonium chloride and extracted with three 100 mL portions of ethyl acetate. The combined organic layers were washed with water and brine and dried over $MgSO_4$. Filtration and concentration in vacuo gave the crude material which was purified by silica gel chromatography to give the desired product as a yellow oil (4.53 g, 63%). ^{1}H NMR (400 MHz, $CDCl_3$) δ 2.35 (s, 3 H), 3.64 (s, 2 H), 3.68 (s, 3 H), 6.99−7.07 (m, 1 H), 7.09−7.14 (m, 1 H), 7.46 (d, J = 2.0 Hz, 1 H), 7.95 (br s, 1 H).

2-(5-Chloro-2-methyl-1*H*-indol-3-yl)acetic Acid (I-20). To a 250 mL round-bottom flask was added **I-19** (4.53 g, 19.07 mmol, 1.0 equiv) and 50 mL of THF. To this was added a solution of lithium hydroxide (2.28 g, 95.37 mmol, 5.0 equiv) in 25 mL of water. To the resulting biphasic mixture was added methanol dropwise until a single layer formed. The resulting solution was stirred for 2 h at room temperature. It was then poured into 1.2 N $HCl_{(aq)}$, and the aqueous layer was extracted with three 100 mL portions of ethyl acetate. The combined organic layers were washed with water and brine and dried over magnesium sulfate. Filtration and removal of solvent in vacuo gave the desired product (3.59 g, 84%). ^{1}H NMR (400 MHz, DMSO-d_6) δ 2.32 (s, 3 H), 3.56 (s, 2 H), 6.98 (dd, J = 8.5, 2.1 Hz, 1 H), 7.25 (d, J = 8.6 Hz, 1 H), 7.40 (d, J = 2.0 Hz, 1 H), 11.05 (s, 1 H), 12.12 (s, 1 H).

2-(2-(5-Chloro-2-methyl-1*H*-indol-3-yl)acetyl)benzoic Acid (I-21). To a 100 mL round-bottom flask under an atmosphere of nitrogen were added **I-20** (3.59 g, 16.13 mmol, 1.0 equiv), phthalic anhydride (2.39 g, 16.13 mmol, 1.0 equiv), and sodium acetate (7.94 g, 96.81 mmol, 6.0 equiv). Then 40 mL of toluene was added, and the suspension was sonicated for 5 min. The toluene was then removed in vacuo and the resulting powder heated neat to 200 °C for 16 h. After the mixture was cooled to room temperature, the resulting brown solid was washed with 1.2 N HCl and water and dried. The resulting material was carried on crude (4.08 g, 77%).

4-((5-Chloro-2-methyl-1*H*-indol-3-yl)methyl)phthalazin-1(2*H*)-one (I-22). To a 500 mL round-bottom flask under an atmosphere of nitrogen were added **I-21** (4.08 g, 12.48 mmol, 1.0 equiv), anhydrous hydrazine (0.78 mL, 24.95 mL, 2.0 equiv), and 250 mL of isopropanol. The resulting mixture was heated to reflux and allowed to stir for 16 h. The solvent was then removed in vacuo and the residue purified by silica gel chromatography to give the desired product as a brown solid (0.755 g, 19%). ^{1}H NMR (400 MHz, DMSO-d_6) δ 2.40 (s, 3 H), 4.32 (s, 2 H), 6.94 (dd, J = 8.5, 2.1 Hz, 1 H), 7.22 (d, J = 8.6 Hz, 1 H), 7.38−7.46 (m, 1 H), 7.75−7.82 (m, 1 H), 7.86 (td, J = 7.6, 1.5 Hz, 1 H), 7.92−7.98 (m, 1 H), 8.24 (dd, J = 7.8, 1.5 Hz, 1 H), 11.06 (s, 1 H), 12.52 (s, 1 H).

2-Benzyl-4-((5-chloro-2-methyl-1*H*-indol-3-yl)methyl)-phthalazin-1(2*H*)-one (I-23). To a 100 mL round-bottom flask under a nitrogen atmosphere were added **I-22** (0.755 g, 2.34 mmol, 1.0 equiv), benzyl bromide (0.56 mL, 4.67 mmol, 2.0 equiv), potassium carbonate (0.806 g, 5.84 mmol, 2.5 equiv), and 50 mL of DMF. The resulting suspension was heated to 85 °C for 16 h. The mixture was then allowed to cool to room temperature and then poured into 200 mL of water. This was extracted with three 50 mL portions of ethyl acetate. The combined organic layers were washed with water and brine and dried over $MgSO_4$. Filtration and concentration in vacuo gave a tan solid. The crude material was purified by silica gel chromatography to give a white solid (0.200 g, 21%).

Methyl 2-(3-((3-Benzyl-4-oxo-3,4-dihydrophthalazin-1-yl)-methyl)-5-chloro-2-methyl-1*H*-indol-1-yl)acetate (I-24). To a 100 mL round-bottom flask under a nitrogen atmosphere was added **I-23** (0.128 g, 0.31 mmol, 1.0 equiv), methyl bromoacetate (0.11 mL, 1.24 mmol, 4.0 equiv), potassium carbonate (0.256 g, 1.86 mmol, 6.0 equiv), and 50 mL of DMF. The resulting suspension was heated to 85 °C for 16 h. The mixture was then allowed to cool to room temperature and then poured into 200 mL of water. This was extracted with three 50 mL portions of ethyl acetate. The combined organic layers were washed with water and brine and dried over $MgSO_4$. Filtration and concentration in vacuo gave a tan solid. The crude material was purified by silica gel chromatography to give a white solid (0.081 g, 54%). ^{1}H NMR (400 MHz, $CDCl_3$) δ 0.88 (s, 1 H), 2.25 (s, 3 H), 3.70 (s, 3 H), 4.31 (s, 2 H), 4.74 (s, 2 H), 5.37 (s, 2 H), 6.97−7.13 (m, 2 H), 7.21−7.34 (m, 4 H), 7.44 (dd, J = 8.1, 1.5 Hz, 2 H), 7.55 (d, J = 1.5 Hz, 1 H), 7.62−7.70 (m, 2 H), 7.73−7.81 (m, 1 H), 8.34−8.48 (m, 1 H).

Compound 27. To a 100 mL round-bottom flask was added **I-24** (0.155 g, 0.32 mmol, 1.0 equiv) and 20 mL of THF. To this was added a solution of lithium hydroxide (0.038 g, 1.60 mmol, 5.0 equiv) in 10 mL of water. To the resulting biphasic mixture was added methanol dropwise until a single layer formed. The resulting solution was stirred for 2 h at room temperature. It was then poured into 1.2 N $HCl_{(aq)}$, and the aqueous layer was extracted with three 50 mL portions of ethyl acetate. The combined organic layers were washed with water and

brine and dried over magnesium sulfate. Filtration and removal of solvent in vacuo gave the crude material. This was purified by reverse phase HPLC and the isolated product lyophilized to give a white powder (0.083 g, 55%). ^{1}H NMR (400 MHz, DMSO-d_6) δ 2.32 (s, 3 H), 4.39 (s, 2 H), 4.93 (s, 2 H), 5.30 (s, 2 H), 7.01 (dd, J = 8.7, 2.1 Hz, 1 H), 7.20−7.42 (m, 6 H), 7.52 (d, J = 1.8 Hz, 1 H), 7.83 (m, J = 7.5, 7.5, 7.5, 7.5, 1.6 Hz, 2 H), 7.96 (dd, J = 6.9, 1.1 Hz, 1 H), 8.28 (dd, J = 7.8, 1.5 Hz, 1 H), 13.09 (br s, 1 H). HRMS: calcd for $C_{27}H_{22}ClN_3O_3$ + H^+, 471.134 97 found (ESI-FTMS, $[M + H]^{1+}$ 471.134 87.

hCRTH2 FRET Assay. The cAMP TR-FRET assay was performed by incubating a dilution series of compound concentrations with 30 000 cells per assay well of CHO-K1 cells expressing the recombinant human CRTH2 receptor (Euroscreen, Belgium). Incubations were performed at room temperature for 30 min in the presence of 10 μM forskolin and 10 nM PGD2. The assay buffer used contained 25 mM 4-(2-hydroxyethyl)-1-piperazineethanesulfonic acid (HEPES), pH 7.4, 124 mM sodium chloride, 5 mM potassium chloride, 1.45 mM calcium chloride, 1.25 mM magnesium chloride, 1.25 mM potassium dihydrogen phosphate, 13.3 mM glucose, and 0.5 g/L BSA. Following the 30 min incubation at room temperature, d2-cAMP and europium-labeled antibody supplied with the Hi-Range assay reagent kit (Cisbio, Bedford, MA) were separately diluted into the supplier-provided cell lysis buffer, and each was added to the assay plate, as per the manufacturer's directions. Data were collected on the Envision plate reader (Perkin-Elmer, Waltham, MA) using λ_{ex} = 340 nm and λ_{em} = 615/665. Samples containing cells and DMSO alone were included as a control in order to measure the maximal signal.

Human Eosinophil Shape Change Assay (hEOS). Peripheral blood from healthy human donors, prescreened for having greater than 3% eosinophils, was collected into sodium heparin tubes. Blood was incubated with compound for 10 min at room temperature and then activated with 50 nM PGD2 for 10 min at 37 °C. The reaction was stopped by transferring the plates to ice and adding 1% paraformaldehyde fixative. The samples were then transferred to ammonium chloride lysis solution, mixed gently, and incubated on ice for 40 min. Eosinophil shape change was analyzed by flow cytometry using a FACSCalibur outfitted with a 96-well autosampler. Individual cell populations were separated based on their forward and side scatter properties. Granulocytes were gated and assessed for autofluorescence in the FL1 and FL2 channels. Eosinophils were isolated based on their higher autofluorescence in both channels. Finally shape change was measured by alterations in the mean forward scatter of the eosinophils in response to PGD2.

Contact Hypersensitivity Mouse Ear Model (CHS). Inflammation was measured in the ear skin of mice. One week prior to challenge, mice were sensitized on the shaved abdomen by applying 100 μL of 2% oxazolone made in 100% ethanol. Five days later, baseline ear thickness measurements were taken on the left and right ears using a Mitutoyo micrometer. Compound was given orally prior to challenge. One hour after treatment, the left ears of the mice were challenged topically with 10 μL of 2% oxazolone on the left ear, and as a negative control 10 μL of 100% ethanol on the right ear. Mice received another dose of compound orally 7 h after challenge. The following day (24 h) ear swelling was measured again with the micrometer and the swelling was expressed as postchallenge − prechallenge thickness (Δ) (Student's unpaired t test used for statistical analysis).

House Dust Mite Model: Mouse Model of House Dust Mite-Induced Allergic Airway Disease. Age-matched 6−12 week old female BALB/c mice were obtained from Taconic Farms (Hudson, NY). All in vivo experiments were performed in accordance with animal use protocols approved by Pfizer's Institutional Animal Care and Use Committee. On days 0, 7, and 14 of the protocol mice were anesthetized with isoflurane and received house dust mite extract from *Dermatophagoides pteronyssinus* (HDM, Greer Laboratories, Lenoir, NC). Briefly, 100 μg of HDM extract in 40 μL of saline were instilled intratracheally using a 100 μL Hamilton glass syringe terminated with a 1.5 in. polyethylene catheter mounted on a 30G needle. The catheter was introduced through the animal's vocal cords into the trachea using an otoscope terminated with a 2 mm speculum. When indicated, mice were treated (q.d.) either intraperitoneally with dexamethasone (1 mg/kg) or orally with compound **2** (20 mg/kg). All mice were euthanized by CO_2 asphyxiation on day 17 of the protocol to collect bronchoalveolar lavage (BAL) fluid and various tissue samples for analysis. BAL collection and preparation of lung tissue for histopathology were performed as previously described.[32] Results represent the mean ± SEM. Statistical significance for all results was determined using the Mann−Whitney U test. Results were considered significant for $P < 0.05$.

■ AUTHOR INFORMATION

Corresponding Author

*Phone: (617) 665-5626. E-mail: neelu.kaila@pfizer.com.

Notes

The authors declare no competing financial interest.

■ ACKNOWLEDGMENTS

We thank the DAC group for analytical data. We also thank Professor William Abraham from the Mount Sinai Medical Center at University of Miami, FL, for conducting the sheep studies to explore efficacy of compounds in asthma.

■ ABBREVIATIONS USED

hCRTH2, human chemoattractant receptor homologous molecule expressed on Th2 cells; AHR, airway hyperresponsiveness; LAR, late airway response; EAR, early airway response; FRET, fluorescence resonance energy transfer; BOP, benzotriazol-1-yloxytris(dimethylamino)phosphonium hexafluorophosphate; P_{app}, apparent permeability coefficient; pH, potential hydrogen; PGD2, prostaglandin D2; nM, nanomolar; HDM, house dust mite; BAL, bronchoalveolar lavage; $MgSO_4$, magnesium sulfate; HCl, hydrochloric acid; SEM, standard error of the mean; MED, minimal efficacious dose

■ REFERENCES

(1) (a) Nagata, K.; Hirai, H.; Tanaka, K.; Ogawa, K.; Aso, T.; Sugamura, K.; Nakamura, M.; Takano, S. CRTH2, an orphan receptor of T-helper-2-cells, is expressed on basophils and eosinophils and responds to mast cell-derived factor(s). *FEBS Lett.* **1999**, *459*, 195−199. (b) Nagata, K.; Hirai, H. The second PGD(2) receptor CRTH2: structure, properties, and functions in leukocytes. *Prostaglandins, Leukotrienes Essent. Fatty Acids* **2003**, *69*, 169−177. (c) Kostenis, E.; Ulven, T. Emerging roles of DP and CRTH2 in allergic inflammation. *Trends Mol. Med.* **2006**, *12*, 148−158. (d) Cosmi, L.; Annunziato, F.; Galli, G.; Manetti, R.; Maggi, E.; Romagnani, S. CRTH2: marker for the detection of human Th2 and Tc2 cells. *Adv. Exp. Med. Biol.* **2001**, *495*, 25−29.

(2) Haeggstrom, J. Z.; Rinaldo-Matthis, A.; Wheelock, C. E.; Wetterholm, A. Advances in eicosanoid research, novel therapeutic implications. *Biochem. Biophys. Res. Commun.* **2010**, *21*, 135−139.

(3) Castellani, M. L.; Felaco, M.; Pandolfi, F.; Salini, V.; De Amicis, D.; Orso, C.; Vecchiet, J.; Tete, S.; Ciampoli, C.; Conti, F.; Cerulli, G.; Caraffa, A.; Antinolfi, P.; Cuccurullo, C.; Felaco, P.; Kempuraj, D.; Boscolo, P.; Sabatino, G.; Shaik, Y. B. Mast cells and arachidonic acid cascade in inflammation. *Eur. J. Inflamation* **2009**, *7*, 131−137.

(4) Hirai, H.; Tanaka, K.; Yoshie, O.; Ogawa, K.; Kenmotsu, K.; Takamori, Y.; Ichimasa, M.; Sugamura, K.; Nakamura, M.; Takano, S. Prostaglandin D2 selectively induces chemotaxis in T helper type 2 cells, eosinophils, and basophils via seven-transmembrane receptor CRTH2. *J. Exp. Med.* **2001**, *193*, 255−262.

(5) Huang, J.-L.; Gao, P.-S.; Mathias, R. A.; Yao, T.-C.; Chen, L.-C.; Kuo, M.-L.; Hsu, S.-C.; Plunkett, B.; Togias, A.; Barnes, K. C. Sequence variants of the gene encoding chemoattractant receptor expressed on Th2 cells (CRTH2) are associated with asthma and differentially influence mRNA stability. *Hum. Mol. Genet.* **2004**, *13*, 2691−2697.

(6) (a) Novel, U. T.; Kostenis, E. CRTH2 antagonists: a review of patents from 2006 to 2009. *Expert Opin. Ther. Pat.* **2010**, *20*, 1505–1530. (b) Chen, J. J.; Budelsky, A. L. Prostaglandin D2 receptor CRTH2 antagonists for the treatment of inflammatory diseases. *Prog. Med. Chem.* **2011**, *50*, 49–107.

(7) (a) Barnes, N.; Pavord, I.; Chuchalin, A.; Bell, J.; Hunter, M.; Lewis, T.; Parker, D.; Payton, M.; Collins, L. P.; Pettipher, R.; Steiner, J.; Perkins, C. M. A randomized, double-blind, placebo-controlled study of the CRTH2 antagonist OC000459 in moderate persistent asthma. *Clin. Exp. Allergy* **2012**, *42*, 38–48. (b) Safety and Efficacy Study of OC000459 Dosed Twice Daily for 28 Days in Asthmatic Subjects. http://clinicaltrials.gov/ct2/show/NCT01057927?term=OC000459&rank=4.

(8) *Actelion'S Clinical Development*; Actelion Pharmaceuticals Ltd.: Basel, Switzerland, 2012.http://www.actelion.com/documents/corporate/fact_sheets/FS_ClinicalDevelopment.pdf.

(9) Study To Assess the Efficacy and Safety of AZD1981 in Patients with Moderate to Severe Chronic Obstructive Pulmonary Disease (COPD) (Columbus). http://clinicaltrials.gov/ct2/show/NCT00690482?term=AZD1981&rank=9.

(10) (a) Efficacy, Safety and Pharmacokinetics of QAV680 in Asthma Patients. http://clinicaltrials.gov/ct2/show/NCT00814216?term=qav680&rank=1. (b) Efficacy, Safety and Pharmacokinetics of QAV680 Versus Placebo in Patients with Asthma. http://clinicaltrials.gov/ct2/show/NCT01103037?term=qav680&rank=2.

(11) Available from http://www.clinicaltrials.gov/ct2/show/NCT01018550?term=amg853&rank=1.

(12) Press Release: ABCD Boehringer Ingelheim To Acquire Actimis Pharmaceuticals. http://www.actimis.com/actimisBI6172008.pdf.

(13) (a) Amira Pharmaceuticals Announces Initial Positive Phase 1 Clinical Data for AM211, a Novel Product Candidate for the Treatment of Respiratory Diseases Results. Demonstrate Positive Proof of Mechanism. http://www.amirapharm.com/articles/DP2_Clinical_Announcement_June2009.html. (b) Amira Pharmaceuticals Announces Initial Positive Phase 1 Clinical Data for AM461, a Back-Up to Amira's Lead DP2 Antagonist, AM211. Results Demonstrate Positive Proof of Mechanism. http://www.amirapharm.com/articles/Amira%20AM461%20Clinical%20Announcement.html.

(14) (a) Burgess, L. E. Recent advances in the discovery and development of CRTH2 antagonists. *Annu. Rep. Med. Chem.* **2011**, *46*, 119–134. (b) Bonafoux, D.; Abibi, A.; Bettencourt, B.; Burchat, A.; Ericsson, A.; Harris, C. M.; Kebede, T.; Morytko, M.; McPherson, M.; Wallace, G.; Wu, X. Thienopyrrole acetic acids as antagonists of the CRTH2 receptor. *Bioorg. Med. Chem. Lett.* **2011**, *21*, 1861–1864. (c) Luker, T.; Bonnert, R.; Schmidt, J.; Sargent, C.; Paine, S. W.; Thom, S.; Pairaudeau, G.; Patel, A.; Mohammed, R.; Akam, E.; Dougall, I.; Davis, A. M.; Abbott, P.; Brough, S.; Millichip, I.; McInally, T. Switching between agonists and antagonists at CRTH2 in a series of highly potent and selective biaryl phenoxyacetic acids. *Bioorg. Med. Chem. Lett.* **2011**, *21*, 3616–3621. (d) Luker, T.; Bonnert, R.; Brough, S.; Cook, A. R.; Dickinson, M. R.; Dougall, I.; Logan, C.; Mohammed, R. T.; Paine, S.; Sanganee, H. J.; Sargent, C.; Schmidt, J. A.; Teague, S.; Thom, S. Substituted indole-1-acetic acids as potent and selective CRTH2 antagonists -discovery of AZD1981. *Bioorg. Med. Chem. Lett.* **2011**, *21*, 6288–6292. (e) Liu, J.; Cheng, A. C.; Tang, H. L.; Medina, J. C. Benzodiazepinone derivatives as CRTH2 antagonists. *ACS Med. Chem. Lett.* **2011**, *2*, 515–518. (f) Crosignani, S.; Jorand-Lebrun, C.; Page, P.; Campbell, G.; Colovray, V.; Missotten, M.; Humbert, Y.; Cleva, C.; Arrighi, J.-F.; Gaudet, M.; Johnson, Z.; Ferro, P.; Chollet, A. Optimization of the central core of indolinone-acetic acid-based CRTH2 (DP2) receptor antagonists. *ACS Med. Chem. Lett.* **2011**, *2*, 644–649. (g) Gervais, F. G.; Sawyer, N.; Stocco, R.; Hamel, M.; Krawczyk, C.; Sillaots, S.; Denis, D.; Wong, E.; Wang, Z.; Gallant, M.; Abraham, W. M.; Slipetz, D.; Crackower, M. A.; O'Neill, G. P. Pharmacological characterization of MK-7246, a potent and selective CRTH2 (chemoattractant receptor-homologous molecule expressed on T-helper type 2 cells) antagonist. *Mol. Pharmacol.* **2011**, *79*, 69–76. (h) Crosignani, S.; Pretre, A.; Jorand-Lebrun, C.; Fraboulet, G.; Seenisamy, J.; Augustine, J. K.; Missotten, M.; Humbert, Y.; Cleva, C.; Abla, N.; Daff, H.; Schott, O.; Schneider, M.; Burgat-Charvillon, F.; Rivron, D.; Hamernig, I.; Arrighi, J.-F.; Gaudet, M.; Zimmerli, S. C.; Juillard, P.; Johnson, Z. Discovery of potent, selective, and orally bioavailable alkynylphenoxyacetic acid CRTH2 (DP2) receptor antagonists for the treatment of allergic inflammatory diseases. *J. Med. Chem.* **2011**, *54*, 7299–7317. (i) Pettipher, R.; Whittaker, M. Update on the development of antagonists of chemoattractant receptor-homologous molecule expressed on Th2 cells (CRTH2). From lead optimization to clinical proof-of-concept in asthma and allergic rhinitis. *J. Med. Chem.* **2012**, *55*, 2915–2931. (j) Ito, S.; Terasaka, T.; Zenkoh, T.; Matsuda, H.; Hayashida, H.; Nagata, H.; Imamura, Y.; Kobayashi, M.; Takeuchi, M.; Ohta, M. Discovery of novel and potent CRTH2 antagonists. *Bioorg. Med. Chem. Lett.* **2012**, *22*, 1194–1197. (k) Crosignani, S.; Jorand-Lebrun, C.; Campbell, G.; Pretre, A.; Grippi-Vallotton, T.; Quattropani, A.; Bouscary-Desforges, G; Bombrun, A.; Missotten, M.; Humbert, Y.; Fremaux, C.; Paquet, M.; El Harkani, K.; Bradshaw, C. G.; Cleva, C.; Abla, N.; Daff, H.; Schott, O.; Pittet, P.-A.; Arrighi, J.-F.; Gaudet, M.; Johnson, Z. Discovery of a novel series of CRTH2 (DP2) receptor antagonists devoid of carboxylic acids. *ACS Med. Chem. Lett* **2011**, *2*, 938–942.

(15) Bennani, Y. L.; Tumey, L. N.; Gleason, E. A.; Robarge, M. J. Indole Acetic Acids Exhibiting CRTH2 Receptor Antagonism and Their Preparation, Pharmaceutical Compositions, and Uses for Treatment of Diseases Responsive to Binding Inhibition of Prostaglandin D2 and Its Metabolites to the CRTH2 Receptor. WO 2006034419 A2, 2006.

(16) Pal, M.; Batchu, V. R.; Parasuraman, K.; Yeleswarapu, K. R. Aluminum chloride-induced heteroarylation of arenes and heteroarenes. 2. A new synthesis of 4-substituted phthalazin-1(2*H*)-ones. *J. Org. Chem.* **2003**, *68*, 6806–6809.

(17) Zhu, W.; Ma, D. Synthesis of aryl sulfones via L-proline-promoted CuI-catalyzed coupling reaction of aryl halides with sulfinic acid salts. *J. Org. Chem.* **2005**, *70*, 2696–2700.

(18) Stoll, A. H.; Knochel, P. Preparation of fully substituted anilines for the synthesis of functionalized indoles. *Org. Lett.* **2008**, *10*, 113–116.

(19) Ezquerra, J.; Pedregal, C.; Lamas, C.; Barluenga, J.; Perez, M.; Garcia-Martin, M. A.; Gonzalez, J. M. Efficient reagents for the synthesis of 5-, 7-, and 5,7-substituted indoles starting from aromatic amines: scope and limitations. *J. Org. Chem.* **1996**, *61*, 5804–5812.

(20) Kuyper, L. F.; Baccanari, D. P.; Jones, M. L.; Hunter, R. N.; Tansik, R. L.; Joyner, S. S.; Boytos, C. M.; Rudolph, S. K.; Knick, V.; Wilson, H. R.; Caddell, J. M.; Friedman, H. S.; Comley, J. C. W.; Stables, J. N. High-affinity inhibitors of dihydrofolate reductase: antimicrobial and anticancer activities of 7,8-dialkyl-1,3-diaminopyrrolo[3,2-*f*]quinazolines with small molecular size. *J. Med. Chem.* **1996**, *39*, 892–903.

(21) Mahadevan, A.; Sard, H.; Gonzalez, M.; McKew, J. C. A general method for C3 reductive alkylation of indoles. *Tetrahedron Lett.* **2003**, *44*, 4589–4591.

(22) Purchased from Apollo Scientific, U.K.

(23) Olsen, A. G.; Dahl, O.; Nielsen, P. E. Synthesis and evaluation of a conformationally constrained pyridazinone PNA-monomer for recognition of thymine in triple-helix structures. *Bioorg. Med. Chem. Lett.* **2004**, *14*, 1551–1554.

(24) The passive permeability model is an in-house computational model. The predicted value is apparent permeability at pH 7.4, reflecting the velocity of molecule passage through a membrane barrier. The unit is 10^{-6} cm/s where higher values indicate greater permeability.

(25) Hammad, H.; Chieppa, M.; Perros, F.; Willart, M. A.; Germain, R. N.; Lambrecht, B. N. House dust mite allergen induces asthma via Toll-like receptor 4 triggering of airway structural cells. *Nat. Med.* **2009**, *15*, 410–416.

(26) (a) Abraham, W. M.; Ahmed, A.; Sabater, J. R.; Lauredo, I. T.; Botvinnikova, Y.; Bjercke, R. J.; Hu, X.; Revelle, B. M.; Kogan, T. P.; Scott, I. L. Selectin blockade prevents antigen-induced late bronchial responses and airway hyperresponsiveness in allergic sheep. *Am. J.*

Respir. Crit. Care Med. **1999**, *159*, 1205−1214. (b) Abraham, W. M. Modeling of asthma, COPD and cystic fibrosis in sheep. *Pulm. Pharmacol. Ther.* **2008**, *21*, 743−754.

(27) Zhu, W.; Ma, D. Synthesis of aryl sulfones via L-proline-promoted CuI-catalyzed coupling reaction of aryl halides with sulfinic acid salts. *J. Org. Chem.* **2005**, *70*, 2696−2700.

(28) (a) Bennasar, M. L.; Roca, T.; Griera, R.; Bassa, M.; Bosch, J. Generation and intermolecular reactions of 3-indolylacyl radicals. *J. Org. Chem.* **2002**, *67*, 6268−6271. (b) Kagayama, K.; Morimoto, T.; Nagata, S.; Katoh, F.; Zhang, X.; Inoue, N.; Hashino, A.; Kageyama, K.; Shikaura, J.; Niwa, T. Synthesis and biological evaluation of novel phthalazinone derivatives as topically active phosphodiesterase 4 inhibitors. *Bioorg. Med. Chem.* **2009**, *17*, 6959−6970.

(29) Demko, Z. P.; Sharpless, K. B. Preparation of 5-substituted 1*H*-tetrazoles from nitriles in water. *J. Org. Chem.* **2001**, *66*, 7945−7950.

(30) Beaulieu, C.; Wang, Z.; Denis, D.; Greig, G.; Lamontagne, S.; O'Neill, G.; Slipetz, D.; Wang, J. Benzimidazoles as new potent and selective DP antagonists for the treatment of allergic rhinitis. *Bioorg. Med. Chem. Lett.* **2004**, *14*, 3195−3199.

(31) Franzke, A.; Pfaltz, A. Synthesis of functionalized borate building blocks for the anionic derivatization of neutral compounds. *Synthesis* **2008**, 245−252.

(32) Long, A. J.; Sypek, J. P.; Askew, R.; Fish, S. C.; Mason, L. E.; Williams, C. M.; Goldman, S. J. Gob-5 contributes to goblet cell hyperplasia and modulates pulmonary tissue inflammation. *Am. J. Respir. Cell Mol. Biol.* **2006**, *35*, 357−365.